water

MDPI

Article

Monitoring of Calcite Precipitation in Hardwater Lakes with Multi-Spectral Remote Sensing Archives

Iris Heine [1,*], Achim Brauer [2], Birgit Heim [3], Sibylle Itzerott [1], Peter Kasprzak [4], Ulrike Kienel [2,5] and Birgit Kleinschmit [6]

1 Helmholtz Centre Potsdam, GFZ German Research Centre for Geosciences, Section 1.4 Remote Sensing, Telegrafenberg, 14473 Potsdam, Germany; itzerott@gfz-potsdam.de
2 Helmholtz Centre Potsdam, GFZ German Research Centre for Geosciences, Section 5.2 Climate Dynamics and Landscape Evolution, Telegrafenberg, 14473 Potsdam, Germany; brau@gfz-potsdam.de (A.B); ukienel@gfz-potsdam.de (U.K.)
3 Alfred Wegener Helmholtz Center for Polar and Marine Research, Telegrafenberg, 14473 Potsdam, Germany; Birgit.Heim@awi.de
4 Department of Experimental Limnology, Leibniz-Institute of Freshwater Ecology & Inland Fisheries, Alte Fischerhütte 2, OT Neuglobsow, 16775 Stechlin, Germany; daphnia@igb-berlin.de
5 Institute for Geography and Geology, University Greifswald, Friedrich-Ludwig-Jahn-Street 16, 17487 Greifswald, Germany
6 Geoinformation in Environmental Planning Lab, Technische Universität Berlin, Straße des 17. Juni 145, 10623 Berlin, Germany; birgit.kleinschmit@tu-berlin.de
* Correspondence: iheine@gfz-potsdam.de; Tel.: +49-331-288-1763; Fax: +49-331-288-1192

Academic Editor: Y. Jun Xu
Received: 4 October 2016; Accepted: 13 December 2016; Published: 3 January 2017

Abstract: Calcite precipitation is a common phenomenon in calcium-rich hardwater lakes during spring and summer, but the number and spatial distribution of lakes with calcite precipitation is unknown. This paper presents a remote sensing based method to observe calcite precipitation over large areas, which are an important prerequisite for a systematic monitoring and evaluation of restoration measurements. We use globally archived satellite remote sensing data for a retrospective systematic assessment of past multi-temporal calcite precipitation events. The database of this study consists of 205 data sets that comprise freely available Landsat and Sentinel 2 data acquired between 1998 and 2015 covering the Northeast German Plain. Calcite precipitation is automatically identified using the green spectra and the metric BGR area, the triangular area between the blue, green and red reflectance value. The validation is based on field measurements of $CaCO_3$ concentrations at three selected lakes, Feldberger Haussee, Breiter Luzin and Schmaler Luzin. The classification accuracy (0.88) is highest for calcite concentrations $\geq$0.7 mg/L. False negative results are caused by the choice of a conservative classification threshold. False positive results can be explained by already increased calcite concentrations. We successfully transferred the developed method to 21 other hardwater lakes in Northeast Germany. The average duration of lakes with regular calcite precipitation is 37 days. The frequency of calcite precipitation reaches from single time detections up to detections nearly every year. False negative classification results and gaps in Landsat time series reduce the accuracy of frequency and duration monitoring, but in future the image density will increase by acquisitions of Sentinel-2a (and 2b). Our study tested successfully the transfer of the classification approach to Sentinel-2 images. Our study shows that 15 of the 24 lakes have at least one phase of calcite precipitation and all events occur between May and September. At the lakes Schmaler Luzin and Feldberger Haussee, we illustrated the influence of ecological restoration measures aiming at nutrient reduction in the lake water on calcite precipitation. Our study emphasizes the high variance of calcite precipitation in hardwater lakes: each lake has to be monitored individually, which is feasible using Landsat and Sentinel-2 time series.

Keywords: calcium-rich hardwater lakes; Landsat Time series analysis; Sentinel 2; Northeast German Plain; evaluation of ecological restoration measures

1. Introduction

Calcite (or calcium carbonate) precipitation events in lakes are a common phenomenon in calcium-rich hardwater lakes. They are also described as "whiting", "milky water phenomenon" or "seasonal clouding" [1–3]. The complex process of calcite precipitation has been intensively studied [1,3–19].

Calcite precipitation is the consequence of the supersaturation of the lake water with respect to calcite. Principally, two possible mechanisms can lead to supersaturation: (1) physical-chemical, through seasonal temperature effects on the solubility of carbon dioxide and calcite (i.e., the solubility of calcite decreases with increasing temperature); and (2) biogenic induction through assimilation of carbon dioxide by plankton blooms of photosynthesizing algae and bacteria in the phototrophic upper water column [2,9] with impact on the carbonate equilibria of the water, which varies with pH, alkalinity, and total dissolved carbon. Aside from that, cells of algae and cyanobacteria can act as surface catalysts for calcite precipitation well before supersaturation is reached [17,18]. In line with that, calcite precipitation events in lakes are recorded after peak phytoplankton blooms [13,16,17]. Calcite precipitation was found to intensify in relation with the trophic state (based on the concentration of dissolved P) from oligotrophic towards weakly eutrophic conditions, but became weaker towards hypereutrophic/polytrophic conditions because of the inhibition of the precipitation by increased P concentration [14–16].

The Northeast German Plain is a region dominated by many hardwater lakes [3]. Studies concerning these lakes showed that calcite precipitation is an important variable impacting on both the water quality and the ecology of these ecosystems [3,5,6]. Calcite precipitation reduces the nutrient concentration and, consequently, phytoplankton productivity and therefore is a natural protection mechanism of hardwater lakes against eutrophication [3,5]. The reduction of nutrient concentration ("self-cleaning") is caused by the co-precipitation of soluble inorganic phosphorus and the flocculation of particles containing phosphorus, which are eventually transported to the sediment at the bottom of a respective lake [3,20]. In times of climate change, also the storage of CO_2 in the sediments might be an important factor. A study at lake Breiter Luzin in Mecklenburg-Vorpommern, Germany, specified sedimentation rates of 300 g $CaCO_3/m^2/day$ [3] and Koschel et al. estimate a calcite production and sedimentation of 150–900 ton/km^2 per year for seven lakes in Mecklenburg-Vorpommern [6]. Whereas precipitated calcite resuspends to some extent, the majority sinks to the lake bottom [12] and is, without mixing, accumulated in calcite layers. Those calcite sediments have been used for the reconstruction of past precipitation events in other regions [20,21]. However, although the ecological importance of calcite precipitation is recognized, neither the number of lakes with calcite precipitation in the Northeast German Plain nor worldwide is known, because only individual lakes are monitored regularly [3,5,6]. Additionally, calcite precipitation varies both within and among lakes: intensity, frequency and duration of calcite precipitation events can vary from year to year [6]. Thus, calcite precipitation events may easily be missed during one-time observations or short-term monitoring of lakes. Here, remote sensing archives of optical satellite missions such as Landsat or Sentinel offer a great potential for a satellite-based long-term monitoring of lakes with high temporal and spatial resolution and for the synoptic monitoring of a larger region like the Northeast German Plain.

However, only few studies have used remote sensing for the monitoring of calcite precipitation. In southwest Florida and Great Bahama Bank whitings have been monitored using medium-resolution MODIS imagery [22,23] and photographs from the NASA manned spacecraft program [24]. Two studies have been conducted on the spatial distribution of calcite precipitation within large lakes (the Great Lakes, and Lake Constance) with Landsat imagery [1,25] and Thiemann and Koschel classified calcite precipitation in 21 lakes in the Northeast German Plain using one hyperspectral airborne data set [2].

In our study, we exploit the multi-spectral long-term remote sensing archive of Landsat and test the applicability for the recently started Sentinel-2 for the long-term monitoring of calcite precipitation in the Northeast German Plain. In this context, the objectives of this study are:

- To develop a robust automated remote sensing-based approach for retrospective long-term multi-temporal calcite precipitation monitoring based on a multi-sensor remote sensing time series.
- To characterize calcite precipitation in terms of frequency and duration to deepen the process understanding.

2. Study Area

The lakes of the Northeast German Plain were formed during the late Weichselian glaciation [3]. We selected three representative study areas: Feldberg Lake District, the Klocksin Lake Chain, and Rheinsberg Lake Region which are located in the federal states of Mecklenburg-Western Pomerania and Brandenburg in Germany (Figure 1). These regions are covered by the Landsat acquisition tiles 193023 and 194023. We chose three lakes with regular in situ measurements in the Feldberg Lake District (Feldberger Haussee, Breiter Luzin, and Schmaler Luzin) for the development of a calcite precipitation classification approach and its validation. Then, the applicability has been tested on the other two regions, the Klocksin Lake Chain and Rheinsberg Lake Region.

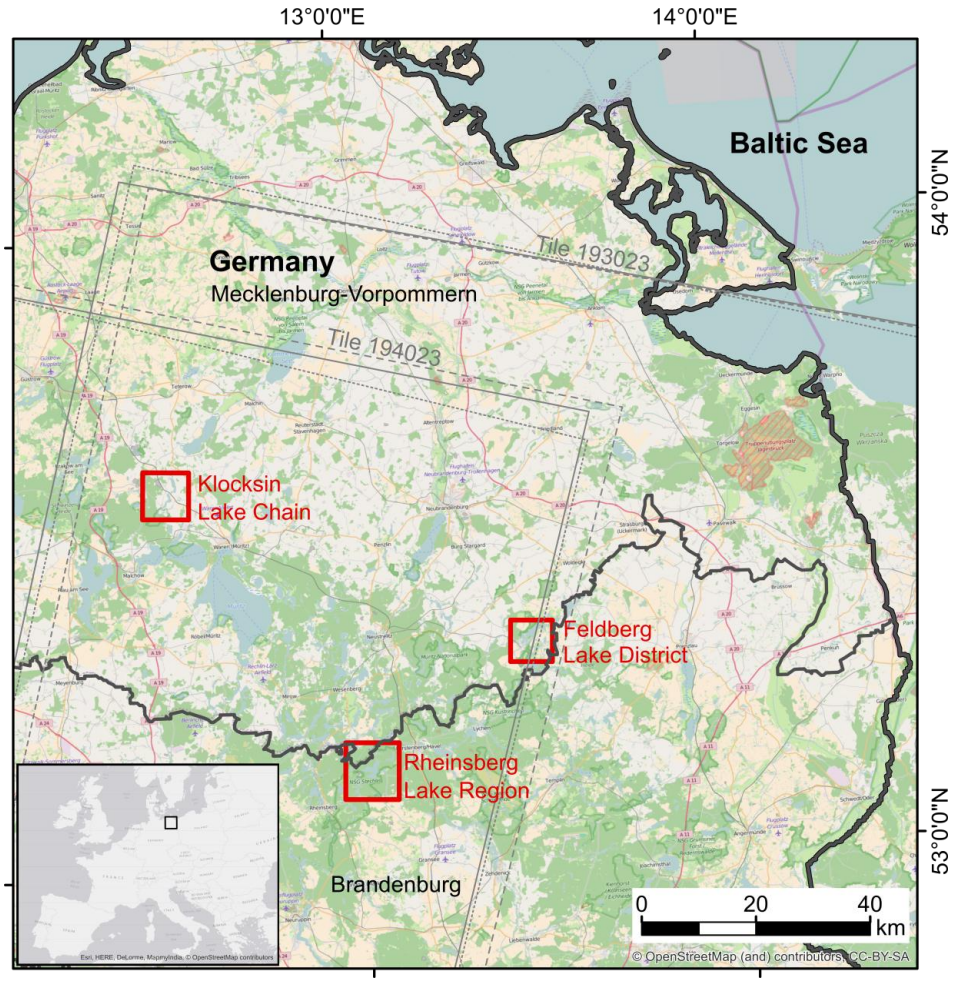

Figure 1. Study area with three selected regions: Feldberg Lake District, the Klocksin Lake Chain, and Rheinsberg Lake Region. The gray lines illustrate the Landsat footprints of the acquisition tiles 193023 and 194023. The gray dashed line shows the footprint of Landsat 5, the solid gray line shows the footprint of Landsat 7, the dotted gray line the footprint of Landsat 8.

2.1. Feldberg Lake District

Figure 2 shows the Feldberg Lake District with its well-researched lakes: Feldberger Haussee (FH), Breiter Luzin (BL) and Schmaler Luzin (SL). All three lakes are hardwater lakes with regular in situ measurements since 1998. The topography, morphology and limnological characteristics of the lakes are summarized in Table 1.

FH potentially used to be a mesotrophic lake, but nutrient input by sewage (phosphorus and nitrogen) and surface runoff since the 1960s until 1980 caused strong eutrophication [26]. In 1980, the sewage discharge was stopped decreasing the external nutrient loading of the lake by 90%. However, because of the tremendous amounts of nutrients (especially phosphorus) stored in the sediment the lake did not respond with a substantial improvement of water quality for decades [27]. Therefore, phosphorus inactivation by treating the lake with poly-aluminum chloride as a flocculation agent was implemented in April 2011. The following drastic reduction of average total phosphorus concentration in the mixed layer from 0.060 mg/L (2006–2010) to 0.017 mg/L (2011–2015) resulted in an improvement of the trophic status from eutrophic to mesotrophic [28,29].

BL is located immediately downstream of FH. BL is known for calcite precipitation [3,5,6]. Its LAWA trophic index of 1997 is mesotrophic, and its potential natural trophy is oligotrophic [30]. An unpublished study of the Leibniz-Institute of Freshwater Ecology & Inland Fisheries (IGB) classified BL in 2015 as mesotrophic.

SL is potentially oligotrophic, but nutrient input lead to a moderate eutrophic state since the 1950s [30]. Since the 1980s the catchment was restored by reducing the nutrient input from the catchment [30], but only a lake restoration in 1996/1997 reduced the eutrophication significantly [12]. The lake was restored by artificially triggering calcite precipitation through in-depth aeration and the addition of $Ca(OH)_2$ in the hypolimnion which caused a significant decrease of total phosphorus content [30]. SL is classified as mesotrophic since 1995, with oligotrophic phases [30,31].

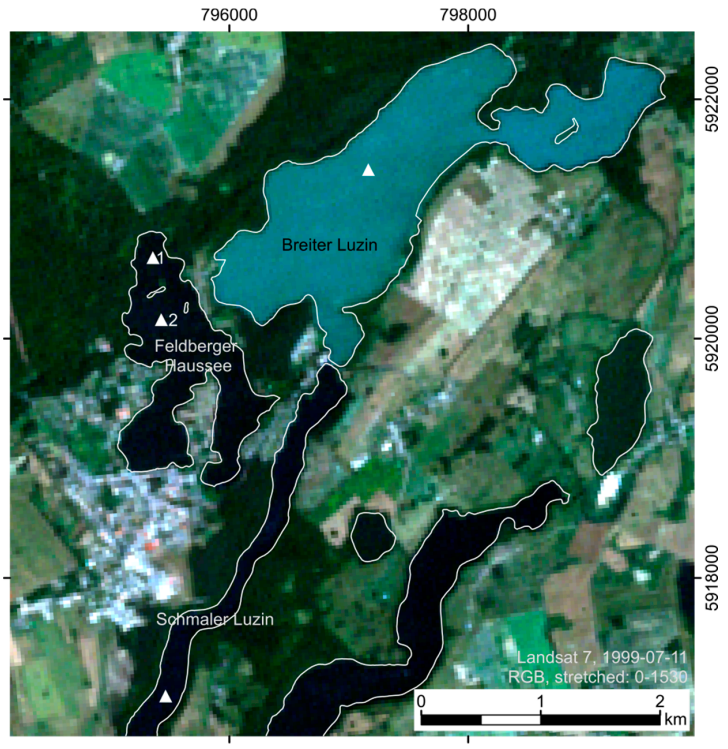

Figure 2. Study area of the Feldberg Lake District on 11 July 1999 (Landsat 7, RGB quasi-true color) with Feldberger Haussee (FH), Breiter Luzin (BL) and Schmaler Luzin (SL). BL has a distinct turquoise color whereas FH and SL are dark blue. All lakes are framed with white lines. The sampling sites are illustrated as white triangles.

For FH, regular calcite precipitation events are documented since 1985. Nevertheless, their intensity (i.e., calcite concentration) clearly increased since the year 2006 and remained high ever since. That was the period when FH finally approached mesotrophic conditions. Koschel (1987) concluded that the intensity of calcite precipitation may be highest in moderately nutrient-enriched hard water lakes, because photosynthesis is high enough to shift the lime-carbonic acid equilibrium to the carbonate side, while the impact of factors to impair the growth of calcite crystals is minimal [3].

Table 1. Overview of morphology and limnological characteristics of the lakes FH, BL, and SL. The limnological characterization is based on the Bund/Länder-Arbeitsgemeinschaft Wasser (LAWA) trophic index.

Lake	Area (km^2) [32]	Maximum Depth (m) [30]	Mean Depth (m) [30]	LAWA 1997 [30]	Trophic Reference State [30]
FH	1.29	12.5	4.9	Eutrophic	Mesotrophic
BL	3.41	58.3	22.3	Mesotrophic	Oligotrophic
SL (without Carwitzer Becken)	0.84	22.5	12.2	Mesotrophic	Oligotrophic

2.2. Klocksin Lake Chain

The second case study area is the Klocksin Lake Chain with Flacher See (FS), Tiefer See (TS), Hofsee (HS), and Bergsee (BS) as shown in Figure 3. There are no regular in situ measurements of $CaCO_3$ concentrations in the lakes, but measurements in 1996 in TS, FS, and BG show high Ca concentrations [30]. The sediment record of TS shows calcite layers in each year and in some years, even two sub layers can be detected during thin section inspection. The calcite layers of the years 1998, 1999, 2003, 2004, 2006, 2007, 2011, and 2012 are thinner than those of the other years in the period considered in this study [33]. This hints at shorter or less intensive calcite precipitation, but dissolution of calcite particles on their way through the water column may also play a role. Analyses of sediment trap material (since 2012) indicate peak calcite precipitation either in May/June and August/September or centered in July [34]. The known topography, morphology and limnological characteristics of the lakes are summarized in Table 2.

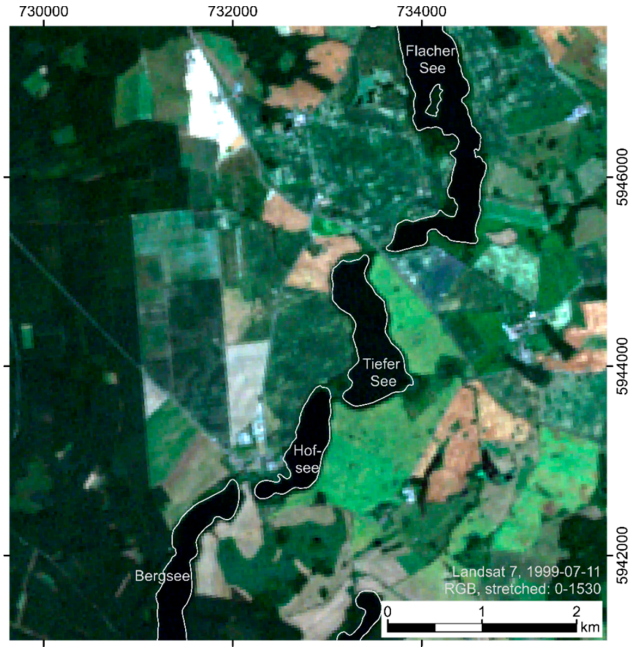

Figure 3. Study area of the Klocksin Lake Chain with Flacher See, Tiefer See, Hofsee and Bergsee on 11 July 1999 (Landsat 7, quasi-true color RGB). All lakes appear dark and are framed with white lines.

Table 2. Overview of morphology and limnological characteristics of the lakes in the Klocksin Lake Chain.

Lake	Area (km^2) [32]	Maximum Depth (m) [30,35]	Mean Depth (m)	LAWA 1996 [30,36]	Trophic Reference State [30]
FS	1.25	31.9	9.7	Mesotrophic	Mesotrophic
TS	0.68	62.5	18.5	Mesotrophic	Oligotrophic
HS	0.39	27	-	Mesotrophic	-
BS	0.57	15.0	6.4	Mesotrophic	Mesotrophic

2.3. Rheinsberg Lake Region

The third test area is the Rheinsberg Lake Region, with Stechlinsee as the largest lake (Figure 4). The LAWA trophic state (1998) of Stechlinsee is oligotrophic, which corresponds to the trophic reference state, and the lake has a low phytoplankton biomass [37]. Stechlinsee is known for calcite precipitation [5,6], and there was an extraordinary intensive event in July 2011 [28].

The northern and southern parts of Nehmitzsee have similar chemical and trophic characteristics: the LAWA trophic state in 1997 classify both parts as mesotrophic, which corresponds to the trophic reference state of the lake. Measurements between March and October 2011 showed constant low phytoplankton of $\leq$0.5 mm^3/L biovolume.

The topography, morphology and limnological characteristics of the lakes, if known, are summarized in Table 3.

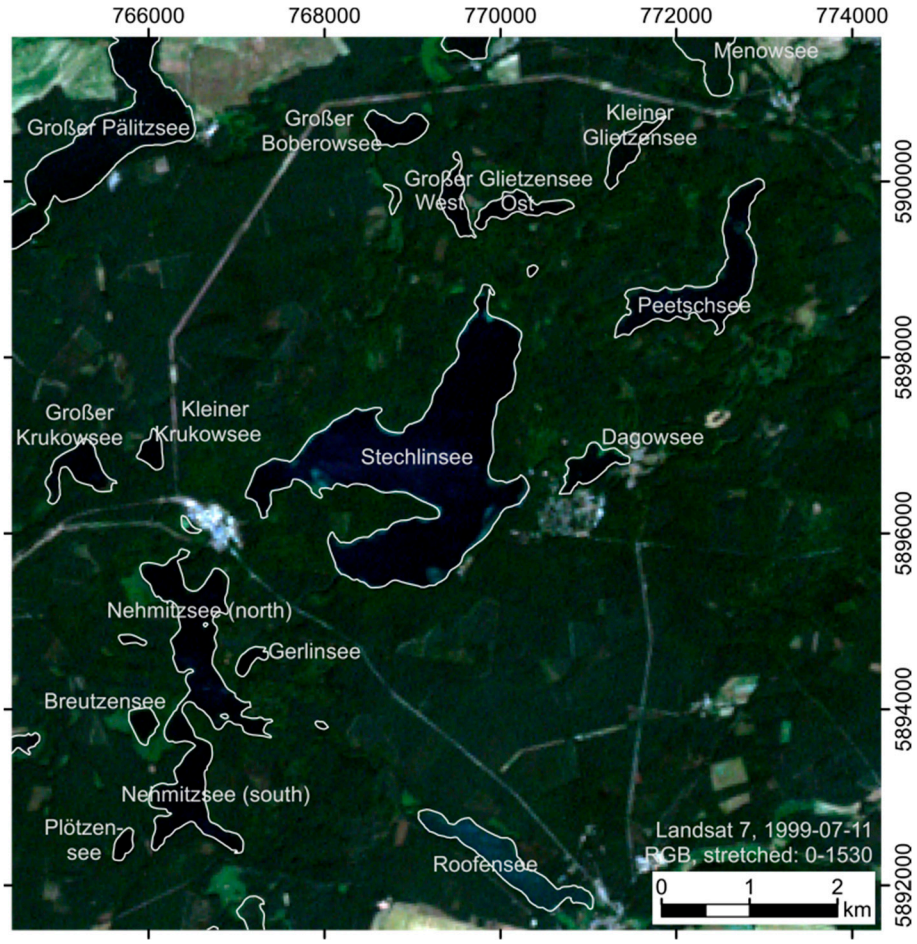

Figure 4. Study area of the Rheinsberg Lake Region on 11 July 1999 (Landsat 7, quasi-true color RGB). All lakes appear dark and are framed with white lines.

Table 3. Overview of morphology and limnological characteristics of the lakes in Rheinsberg Lake Region.

Lake	Area (km^2) [32]	Maximum Depth (m) [35,37–39]	Mean Depth (m) [37,38]	LAWA 1998 [37,39–41]	Trophic Reference State [37]
Breutzensee	0.10	3.5	-	Eutrophic	-
Dagowsee	0.20	9.5	5.0	Eutrophic	-
Gerlinsee	0.06	5.5	-	Mesotrophic	-
Großer Glietzensee (Ost)	0.20	13.0	-	Weakly eutrophic	-
Großer Krukowsee	0.25	13.0	-	Mesotrophic	-
Kleiner Krukowsee	0.08	8.5	-	Mesotrophic	-
Nehmitzsee (north)	1.00	18.6	6.79	Mesotrophic	Mesotrophic
Nehmitzsee (south)	0.64	18.6	6.79	Mesotrophic	Mesotrophic
Peetschsee	0.89	21,0	-	Mesotrophic	-
Plötzensee	0.06	9.0	-	Weakly eutrophic	-
Großer Glietzensee (West)	0.16	10.0	-	Weakly eutrophic	-
Großer Boberowsee	0.18	9.5	-	Eutrophic	-
Großer Pälitzsee	2.49	30	-	Eutrophic	Mesotrophic
Kleiner Glietzensee	0.17	4.0	-	Eutrophic	-
Menowsee	0.35	4.5	-	Mesotrophic	-
Roofensee	0.56	19.0	-	Weakly eutrophic	-
Stechlinsee	4.14	68.0	22.8	Oligotrophic	Oligotrophic

3. Materials and Methods

3.1. Satellite Data and In Situ Data Archive

The multi-temporal satellite remote sensing database comprises data from Landsat 5, 7 and 8 and for 2015 also Sentinel-2 data. The database covers a time span from 1998 to 2015. The repeat cycle of the Landsat satellites is 16 days, the one of Sentinel-2 10 days, but cloud coverage reduces the number of suitable satellite images. The Landsat archives cannot provide a continuous temporal coverage. However, during the years 2003 to 2006 and from 2013 on, high temporal coverage is provided due to the temporal overlap of at least 2 satellite missions. Thus, in this study, the number of suitable Landsat acquisitions varies between 2 and 20 data sets per year with time gaps between 1 day and 160 days between the acquisitions.

In Table 4, we list the bandwidths of the satellites Landsat 5, 7, 8, and Sentinel 2. The visible bands are blue, green, and red and the infrared wavelengths are near-infrared (NIR) and shortwave-infrared (SWIR) 1 and 2. The bands do not overlay perfectly and there are variations in the bandwidths between the sensors. With exception of the NIR band, the old sensors have broader bandwidths: for example, the blue bandwidth ranges between 70 nm to 65 nm, the green between 80 nm and 35 nm and the red between 60 nm and 30 nm.

Table 4. Overview of the bandwidth of the satellites Landsat 5, 7, 8, and Sentinel-2.

	Band Width of Band (nm)						
Satellite	**Blue**	**Green**	**Red**	**NIR**	**SWIR 1**	**SWIR 2**	**Reference**
Landsat 5	450–520	520–600	630–690	760–900	1550–1750	2080–2350	[42]
Landsat 7	450–515	525–605	630–690	775–900	1550–1750	2090–2350	[43]
Landsat 8	450–515	525–600	630–680	845–885	1560–1660	2100–2300	[43]
Sentinel-2	458–523	543–578	650–680	785–900	1565–1655	2100–2280	[44]

The Feldberg Lake District region is covered by 200 Landsat images (60 Landsat 5, 115 Landsat 7, 25 Landsat 8; tiles 193023 and 194023) and by two Sentinel-2 images in 2015. The Klocksin Lake Chain and Rheinsberg Lake Region are covered by additional three Landsat images (one Landsat 7 and two Landsat 8 images, all on tile 194023). The data archive is illustrated in Figure 5.

All the data sets were obtained in the form of orthorectified standard data products to reduce preprocessing efforts. The Landsat images are delivered by U.S. Geological Survey (USGS) as surface reflectance products (including atmospheric correction) [45]. The Sentinel-2 satellite images of region

Feldberg Lake District were provided by ESA in processing level L1C [46]. We did the further preprocessing (resampling and atmospheric correction) with sen2cor (version 2.2.1) and Sentinel-2 Toolbox (version 3.0) provided by ESA [47,48]. The spatial resolution of the data sets ranges from 30 m for the Landsat sensors to 10 m for the Sentinel 2 sensors.

As not all lakes are completely cloud-free, the further preprocessing included the cloud and cloud shadow masking. If not noted differently, all processing was implemented and performed in the free software R (version 3.2.2). The clouds and cloud shadow were removed based on the cloud and cloud shadow classifications that are provided with the data. The cloud and cloud shadow masks of Landsat mask generously, thus, at the Feldberg Lake District, we only use the cloud mask with a high confidence and check for cloud shadows manually to keep the density of the time series in accordance to the in situ data. The Sentinel-2 cloud shadow classification fails over lakes, thus, the images have to be checked manually.

Since 1998, there are regular water quality measurements at FH, BL and SL by the Leibniz-Institute of Freshwater Ecology & Inland Fisheries. Besides precipitated $CaCO_3$, Chlorophyll a (chl-a), temperature, pH, alkalinity, and ion concentrations (NO_3^-, SiO_3^{2-}, Cl^-, SO_4^{2-}, Na^+, K^+, Mg^{2+}, and Ca^{2+}) are measured. Based on those parameters, the $CaCO_3$ saturation index (SI) was calculated according to Debye-Hückel [49] using "WinIAP—Software for the Calculation of Ion Activities and Calcite Saturation Index" [50]. The SI shows, depending on the trophic state and the season, if calcite precipitation is possible: the SI threshold for calcite precipitation in oligotrophic lakes is <5 and in mesotrophic lakes between 5 and 15. In eutrophic lakes, SI values of >15 without calcite precipitation are possible [6]. In spring, the thresholds are generally higher than in summer due to the inhibition of calcite precipitation by phosphate [6].

The locations of measurement stations in the lakes are marked in Figure 2. In FH, $CaCO_3$ is always measured in the northern part of the lake (Figure 2, Δ1) as the other parameters before 2011. Since 2011, the other parameters are measured at another location further south (Figure 2, Δ2). All parameters are measured in 0–5 m water depth and multiple measurements versus depth are averaged.

On 68 days there are water quality measurements contemporary to Landsat images, but not at every time all three lakes are sampled. "Contemporary" in this study means that the Landsat images are not acquired more than 3 days before and not more than 5 days after the in situ measurement. These thresholds are set under the assumption that calcite precipitation events appear more suddenly than they vanish.

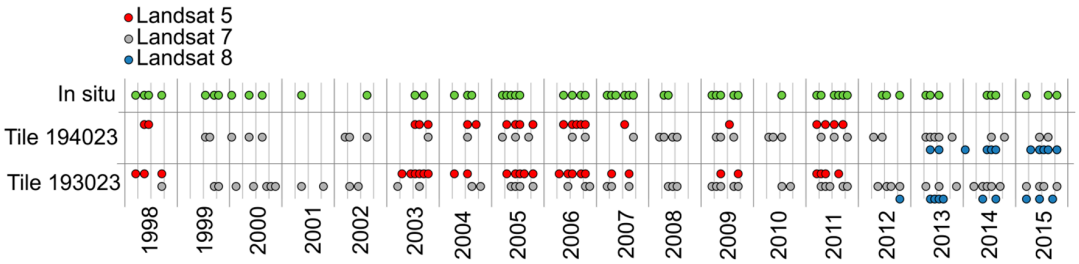

Figure 5. Time series of Landsat acquisitions (1998–2015), sorted by tile (cf. Figure 1) and sensor. "In situ" marks the date of in situ measurements at Feldberg Lake District.

3.2. Classification of Calcite Precipitation Using Satellite Imagery

The processing chain is of the classification is illustrated in Figure 6.

Input data are the preprocessed Landsat and Sentinel images. We manually digitized regions of interest (ROI) for the extraction of lake spectra. For the three lakes of Feldberg Lake District we choose up to 13 ROI per lakes to avoid gaps due to clouds, cloud shadow and the edge of the tile 194023 to keep the density of the satellite data. Thus, those ROI are unevenly distributed in the lakes. At the other lakes we selected one ROI per lake and the ROI are located in the centers of the lakes. All ROI are

selected with distance to islands or shallow water areas, which could influence the reflectance spectra. Depending on the lakes, the ROI are differently sized and shaped.

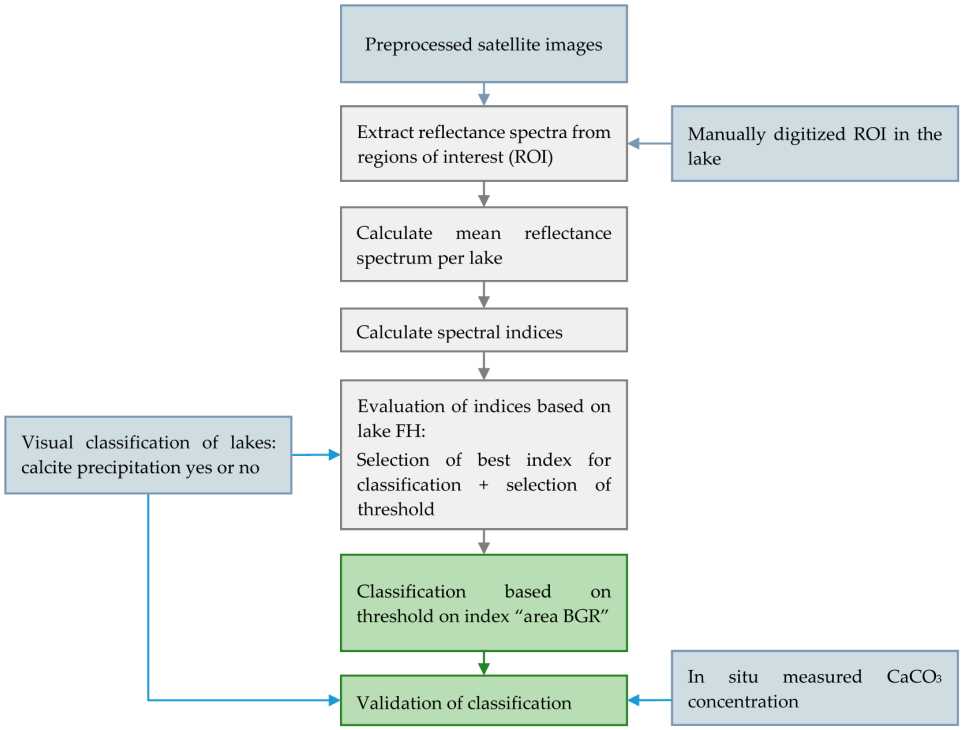

Figure 6. Flowchart of the processing steps of Landsat surface reflectance data for the monitoring of calcite precipitation. The blue boxes contain input data, the gray boxes illustrate the development of the robust classification and the orange boxes illustrate the classification and validation.

Based on the ROI we extracted the reflectance values of the satellite images. The reflectance values are evaluated: if the standard deviation in any band is high (>100) or if more than 10% of the ROI consist of not applicable (NA) values, the next ROI is tested or, if no next ROI is available, the reflectance values of the lake are set NA. Then, the extracted reflectance values of each band are averaged to get the mean reflectance spectrum of the lake.

The next step is the calculation and evaluation of the spectral indices based on the extracted mean reflectance. The spectral indices are described in Table 5.

Table 5. Overview of the spectral indices.

Index Name	Abbreviation	Formula	Reference
Ratio of the reflectance (Ref.) values of band red and green	Ratio RG	$\text{Ratio RG} = \frac{\text{Ref}_{red} - \text{Ref}_{green}}{\text{Ref}_{red} + \text{Ref}_{green}}$	[51]
Normalized difference water index	NDWI	$\text{NDWI} = \frac{\text{Ref}_{green} - \text{Ref}_{NIR}}{\text{Ref}_{green} + \text{Ref}_{NIR}}$	[52]
Modified normalized difference water index	MNDWI	$\text{MNDWI} = \frac{\text{Ref}_{green} - \text{Ref(SWIR1)}}{\text{Ref}_{green} + \text{Ref(SWIR1)}}$	[53]
"Area Blue Green Red" as the triangular area in the reflectance values of blue, green and red (using the central wavelength of Landsat 8 for all sensors)	Area BGR	$\text{Area BGR} = 0.5(482 * \text{Ref}_{green} + 560 * \text{Ref}_{red} + 655 * \text{Ref}_{blue} - 560 * \text{Ref}_{blue} - 655 * \text{Ref}_{green} - 480 * \text{Ref}_{red})$	[54]
Normalized absorption feature depth of red	NAFD	$\text{NAFD} = 1 - \left(\frac{\text{Ref}_{red}}{\text{Ref}_{continumline\_of\_red}} / \text{Area}_{green,red,NIR}\right)$	[55]
Ratio of bands of an unknown lake and a dark reference lake e.g., lake SL	Ratio RL	$\text{Ratio RL} = \frac{\text{Ref}_{unknown\_lake} - \text{Ref}_{reference\_lake}}{\text{Ref}_{unknown\_lake} + \text{Ref}_{reference\_lake}}$	This work

The evaluation of the spectral indices is based on the visual classification of "good quality images" of lake FH: we checked visually the image quality and marked images with a low quality. Reasons for low image quality are large cloud coverage, ice and low incidence angles of the sun in winter. Of the 200 images of Feldberg Lake District 114 have a good image quality. Then, greenish-turquoise colored lakes in a quasi-true color Red Green Blue (RGB) image are classified visually as lakes with calcite precipitation. Finally, each index is separated in two groups, dates with and without calcite precipitation, and the groups are compared.

The validation of the satellite-derived classification results of FH, BL and SL is based on the in situ measured $CaCO_3$ concentrations using confusion matrices. Therefore, the dates with in situ $CaCO_3$ concentrations were classified as "calcite precipitation" and "no calcite precipitation". Additionally, we validate the results based on a visual classification in quasi-true color images. At Feldberg Lake District the visual classification itself is validated using the in situ $CaCO_3$ concentrations. In the other two lake regions without in situ measurements, the satellite-derived calcite precipitation events are only validated with the visual classification in quasi-true color images. Instead of confusion matrices for every lake, we summarize all results of each region and show each region in one confusion matrix. The confusion matrices compare true results, in this study the grouped in situ measurements or visual classification results, with predicted results, in this study the satellite-derived classification results. True positive (TP) and true negative (TN) are accurate classification results, where predicted and true results are equal. False positive (FP) are dates in which the true results show no calcite precipitation, but the satellite-derived calcite precipitation shows calcite precipitation. It means the classification overestimated the number of calcite precipitation. False negative (FN) are dates in which the true results shows calcite precipitation, but the satellite-derived calcite precipitation shows no calcite precipitation. It means the classification underestimated the number of calcite precipitation. The accuracy is calculated by dividing the sum of TP and TN by the sum of TP, TN, FP and FN.

Relevant for the validation with confusion matrices is the number of Landsat images with contemporary in situ measurements, the threshold for the grouping of the in situ $CaCO_3$ concentrations on dates with "calcite precipitation" and "no calcite precipitation", and the relation of dates with calcite precipitation to dates without. FH has 46 dates with Landsat images and field measurements and their $CaCO_3$ concentration ranges from 0 to 3.52 mg/L. BL has 48 dates with Landsat images and field measurements. The $CaCO_3$ concentration ranges from 0.05 to 2.96 mg/L. SL has 31 dates with Landsat images and field measurements and their $CaCO_3$ concentration is always low between 0 and 0.47 mg/L. The number of dates with calcite precipitation varies depending on the $CaCO_3$ that is considered as calcite precipitation. A previous study found that without optical tools, calcite precipitation in the open water is only visible during high calcite concentrations with >1 mg/L [3]. Thus, first, we consider all dates with $CaCO_3$ concentration $\geq$1 mg/L as dates with calcite precipitation. Then, we lower the threshold by 0.1 mg/L steps down to $\geq$0.5 $CaCO_3$ mg/L, because we suspect a higher sensitivity of the satellite images to calcite precipitation.

As algal blooms are potentially a source for misclassification, we also analyze the lake spectra with high chl-a concentration $\geq$20 µg/L. The occurrence of considerable algal blooms are related to an chl-a concentration of at least 20 µg/L [56].

4. Results

4.1. In Situ Measurements

The time series of $CaCO_3$ and SI of the three lakes is illustrated in Figure 7. FH had low $CaCO_3$ concentrations of <1 mg/L before 2006, but exceeded 1 mg/L ten times between 2006 and 2015. BL's $CaCO_3$ concentrations exceeded 1 mg/L twelve times between 1998 and 2015 and SL remained always <0.5 mg/L $CaCO_3$. The SI values of the three lakes range between 0.7 and 13.7 between 2000 and 2015. Based on their SI values and trophic states, in SL and BL calcite precipitation could have occurred during the monitoring period. The trophic state of FH changes during the monitoring period: before

2011 with eutrophic condition no calcite precipitation is possible, after 2011 the SI values indicate possible calcite precipitation events. The chl-a concentration of SL ranges from 1 to 10 µg/L (average: 3 µg/L) and of BL from 1 to 18 µg/L (average: 3 µg/L). FH has high variation in its chl-a concentration: between 1998 and 2002 its chl-a concentration ranges from 4 to 21 µg/L (average: 9 µg/L), then between 2005 and 28 March 2011 it ranges from 5 to 53 µg/L (average: 19 µg/L). After this chl-a maximum, the concentration declines again to 2–17 µg/L (average: 8 µg/L). On twelve dates FH's chl-a concentration exceeds 20 µg/L and thereof, five dates exceed 30 µg/L (23 March 2005, 19 April 2005, 30 May 2008, 30 March 2009, and 28 March 2011).

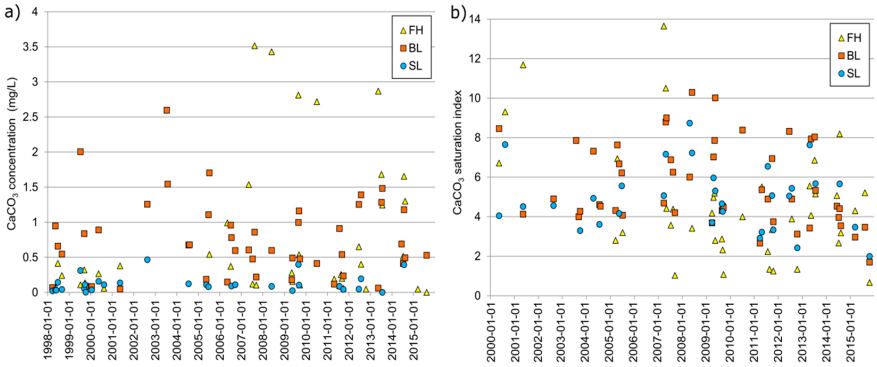

Figure 7. Time series (1998 to 2015) of (**a**) in situ measured $CaCO_3$ concentrations (mg/L); and (**b**) the calculated $CaCO_3$ saturation index (SI) in FH, BL, SL lakes.

4.2. Calcite Precipitation Visible in Lake Reflectance

The methodological developments aim at the automated multi-temporal mapping of calcite precipitation based on satellite remote sensing time series data. Thus, the approach needs to be able to identify calcite precipitation occurring at different times during the analyzed time span, whereas the determination of the time of calcite precipitation occurrence depends on the length of the time period between two subsequent images contained in the remote sensing time series database.

Figure 8 compares two quasi-true color Landsat RGB images, one with [28] and the other without calcite precipitation, with photos from contemporary field campaigns. Figure 9 shows a time series of five Landsat RGB images in which BL has different $CaCO_3$ concentrations. The according mean reflectance spectra and the calculation of Area BGR are shown in Figure 10. On 12 July 1999 the $CaCO_3$ concentration of BL was very high with 2.00 mg/L and the lake is opaque turquoise colored. Until 15 September 1999 the $CaCO_3$ concentrations decreased to 0.84 mg/L, but in the Landsat image the color change is still clearly visible. On 11 October 1999 the calcite precipitation diminished and $CaCO_3$ concentration was very low with 0.09 mg/L and BL appears dark again. The only exceptions are lakes with separated lake basins with narrow passages: On 13 September 1999 the northeastern basin of BL is darker than the main basin (Figure 9d).

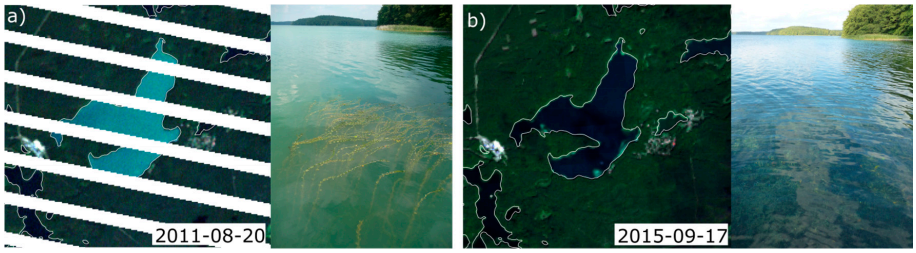

Figure 8. Two quasi-true color Landsat RGB of Stechlinsee with photos showing the water surface taken from a boat: (**a**) August 2011, showing the lake with calcite precipitation; and (**b**) September 2015, with clear water. The photos were taken: (**a**) two days before; and (**b**) nine days after the Landsat acquisition.

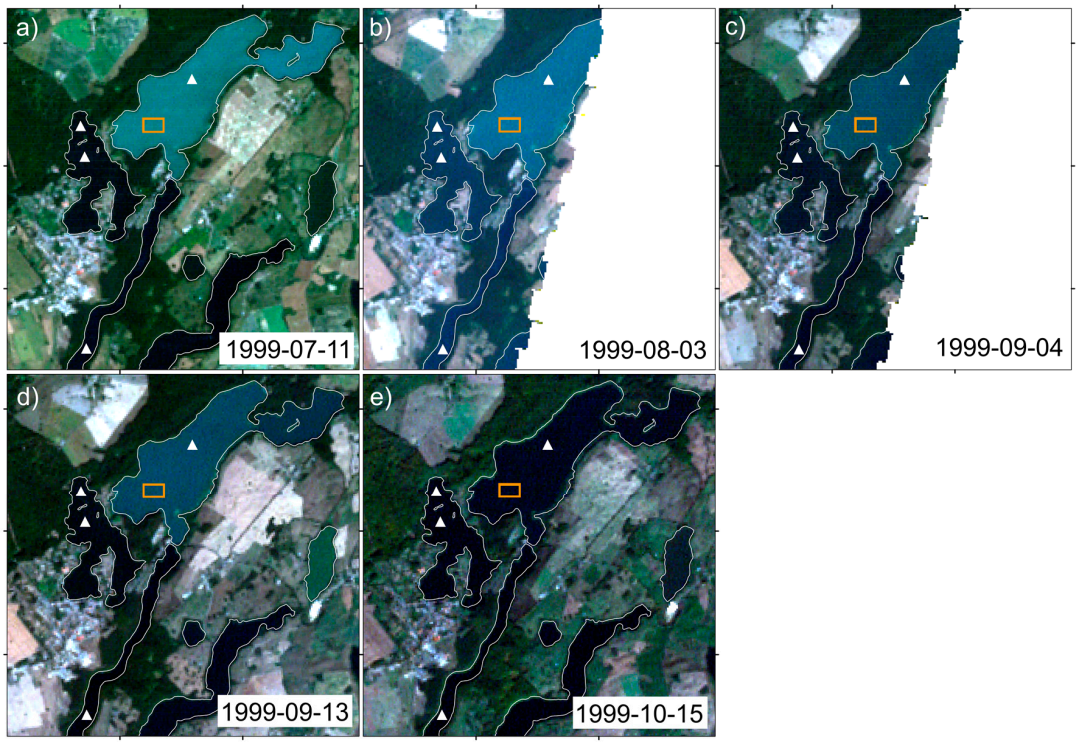

Figure 9. Quasi-true color RGB Landsat 7 images of the Feldberg Lake District. The extent is the same as in Figure 2. All lakes are framed with lines and the positions of in situ measurements are marked with white triangles. The orange rectangle shows the ROI that was used for the extraction of the reflectance spectra. BL is turquoise colored on 11 July 1999 (**a**) due to calcite precipitation. In the following, calcite precipitation diminishes from 3 August 1999 to 13 September 1999 (**b**–**d**), and on 15 October 1999 (**e**) BL appears dark again.

The precipitated $CaCO_3$ particles cause a decrease in Secchi depth and an increase of the reflectance [2,4]. According to Thiemann and Koschel the additive effect of calcite precipitation is uniform in the visible (RGB) and near-infrared wavelength range, so that spectral characteristic like absorption bands and reflection maxima are kept [2]. Figure 10 illustrates the enhanced reflectance values mainly between blue and NIR caused by calcite precipitation. However, the increase varies by wavelength: the green band shows the strongest increase and has the maximum reflectance values. The reference reflectance spectrum without calcite precipitation on 15 October 1999 has low reflectance values with a maximum blue band. Even though the reflectance spectra of calcite precipitation show higher NIR and SWIR reflectance, an analysis above 800 nm is not recommended as the absorption of clear water superimposes the effect of water components [1,2,11,25]. Figure 11 illustrates the variation of lake reflectance spectra with and without calcite precipitation. In the boxplots all mean reflectance spectra of good quality images of BL, SL and FH are combined. With low quality images, the ranges would be even higher. In Figure 11 the mean reflectance values of NIR, SWIR 1, and SWIR 2 do not indicate regular increase of the reflectance, as it could be suspected by the selected reflectance spectra in Figure 10.

There are twelve dates with high chl-a concentration $\geq$20 µg/L at FH. Of the twelve dates with high chl-a concentration, only two show a green color: on 12 April 2005 FH appears greenish in the quasi-true color RGB Landsat 12 April 2005 and on 1 June 2008 FH appears green bright. However, 1 June 2008 has in addition to its high chl-a concentration a calcite precipitation event with a high $CaCO_3$ concentration of 3.4 mg/L. The two lake spectra of FH with greenish/green color are characterized by a steeper increase from blue to green reflectance and a (small) peak in green. The reflectance values of red and NIR are equally high.

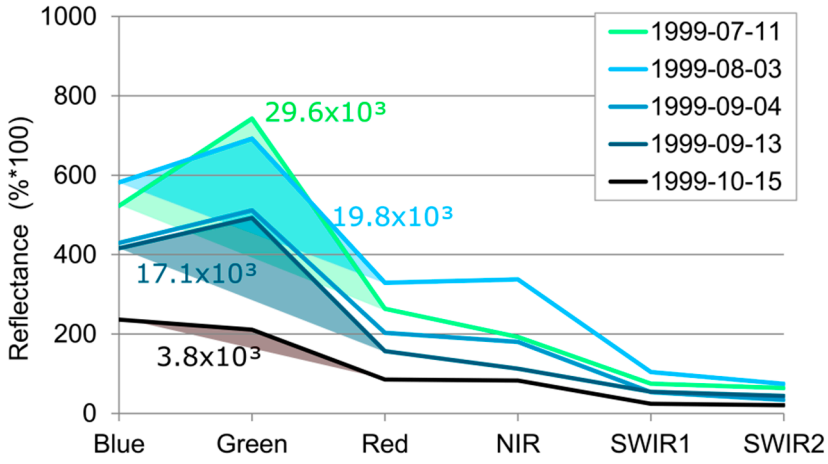

Figure 10. Reflectance spectra of BL with calcite precipitation (11 July 1999), diminishing calcite precipitation (3 August 1999 to 13 September 1999), and without calcite precipitation (15 October 1999). The ROI that has been used for the extraction and calculation of the mean reflectance spectra of BL is marked in Figure 7. The transparent triangles and colored numbers illustrate the "Area BGR".

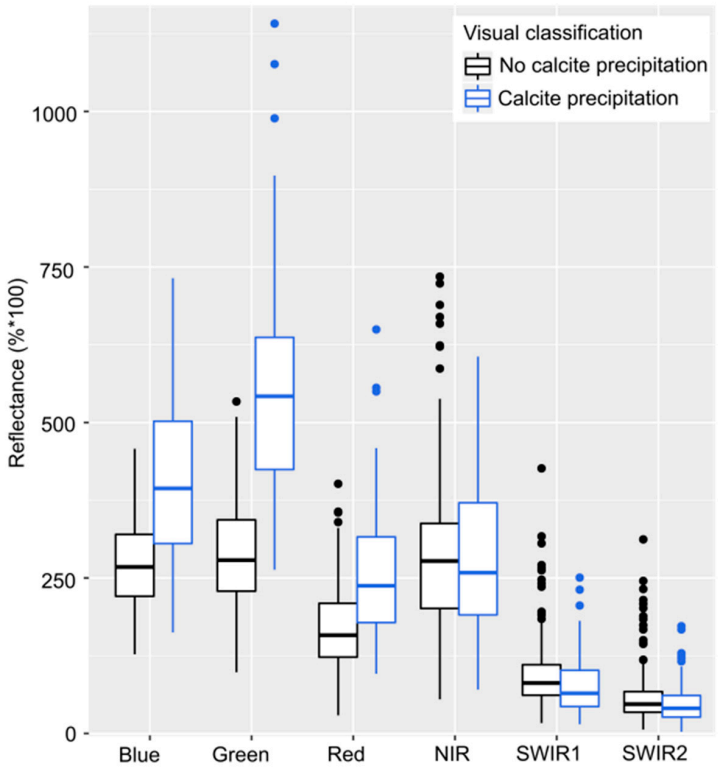

Figure 11. Reflectance values in all spectral bands of Breiter Luzin, Schmaler Luzin and Feldberger Haussee of good quality images. All three lakes are visually classified as turquoise (calcite precipitation) or dark (no calcite precipitation).

4.3. Best Performing Spectral Indices

The evaluation of the green reflectance and the spatial indices of FH is illustrated in Figure 12. Area BGR has clearly the best distinction between the two cases with a 74% increase from 3rd quantile of "no calcite precipitation" to the 1st quantile of the "yes calcite precipitation" boxplot. The next best is the reflectance of green band with 19% increase. We selected a conservative threshold 13×10^3 as the maximum value of dates without calcite precipitation of Area BGR.

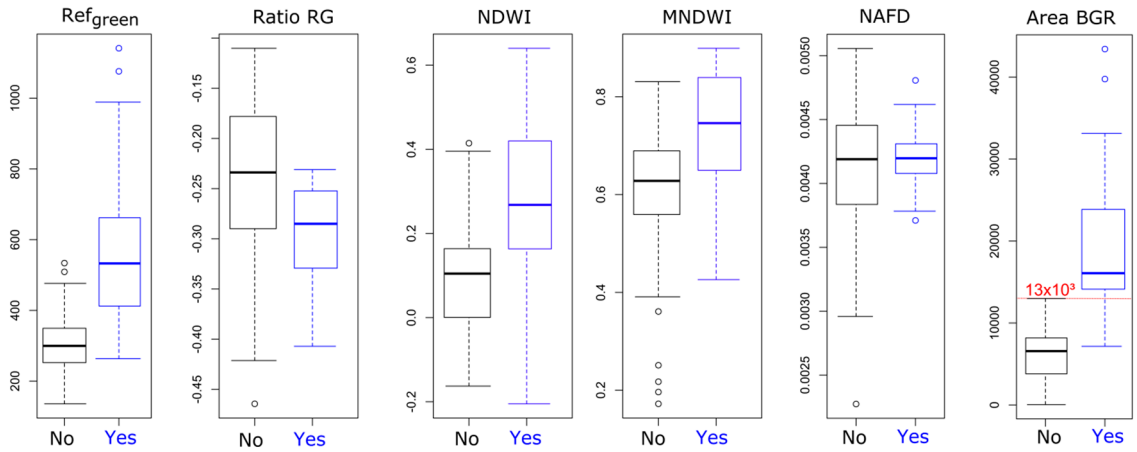

Figure 12. Boxplots of the reflectance of green and the indices of FH of good quality images. The indices are separated into dates with calcite precipitation ("Yes") and without calcite precipitation ("No") based on the visual classification of FH. Index "Area BGR" has the best separation of the two classes: the red line marks the conservative threshold 13×10^3 as the maximum value of dates without calcite precipitation.

The calculation of Ratio RL based on SL failed as soon as no reflectance values of the lake could be extracted, because the area of the lake was masked out in the satellite images due to cloud coverage. It was also not possible to derive a universal reference spectrum, because of the variation of reflectance values of SL. Figure 13 illustrates the variation of the mean spectra of SL, grouped by the satellites. There are large variations within the bands, especially in NIR. Additionally, the reflectance values between the satellites vary: between blue and NIR, Landsat 8 has significantly lower reflectance values than Landsat 5, and the reflectance values of Landsat 7 range between the two other satellites.

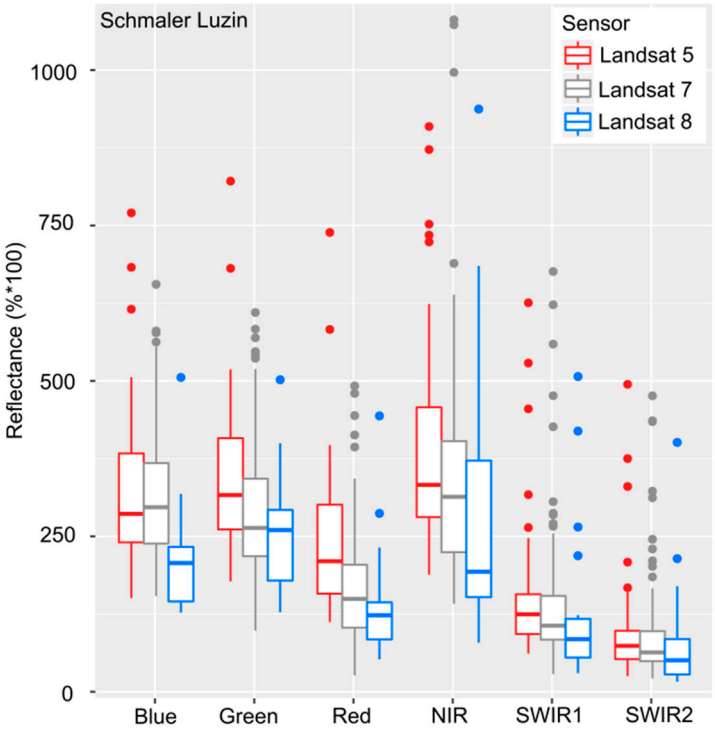

Figure 13. Variation of the mean lake spectra of lake SL between 1998 and 2015. The spectra are grouped by the Landsat satellites.

4.4. Validation of Landsat-Derived Calcite Precipitation

The satellite-derived calcite precipitation of each region was validated using confusion matrices. Table 6 illustrated the number of accurate classification (TP and TF) and misclassified (FN and FP) results at Feldberg Lake District in comparison to in situ measurements of $CaCO_3$ concentration. The classification accuracy depends on the choice of threshold in $CaCO_3$ concentration: the higher the $CaCO_3$ threshold is set, the higher is the number of FP results and the smaller is the number of FN results. The best accuracy of 0.88 has the comparison with the $\geq$0.7 mg/L $CaCO_3$. In that case, FN is six (three at FH and three at BL) and the number of FP is nine (all at BL). The nine false positive dates have (slightly) increased $CaCO_3$ concentrations between 0.41 and 0.69 mg/L.

Table 6. Confusion matrices of Landsat-derived calcite precipitation with in situ measurements at Feldberg Lake District.

$CaCO_3$ Concentration (mg/L)	TP	TN	FN	FP	Sum	Accuracy
$\geq$1	84	21	4	16	125	0.84
$\geq$0.9	82	24	6	13	125	0.848
$\geq$0.8	82	26	6	11	125	0.864
$\geq$0.7	82	28	6	9	125	0.88
$\geq$0.6	78	31	10	6	125	0.872
$\geq$0.5	71	33	17	4	125	0.832

The accuracy of the visual classification is 0.85 using the threshold $\geq$0.7 mg/L $CaCO_3$: the sum is 124, with 75 TP, 31 TN, three FN and 16 FP results.

Table 7 illustrates the accuracies of Feldberg Lake District, Klocksin Lake Chain and Rheinsberg Lake Region using confusion matrices with visual classifications. The accuracy in the Feldberg Lake District is high with 0.94, but with 28 FN and four FP classification results. The FN results occur at all three lakes (FH: 14, BL: 9, and SL: 5), the FN results only at FH (3) and BL (1). The accuracy in the Klocksin Lake Chain is very high with 0.99, with only two FP (at FS) and two FN classification results (at FS and HS). The accuracy in Rheinsberg Lake Region is also high with 0.97; however, there are 54 false negative results. The FN results are two times at Breutzensee and kleiner Glietzensee, four times at Dagowsee and Großer Boberowsee, six times at Stechlinsee, eight times at Großer Pälitzsee and Roofensee, and 20 times at Menowsee. Even though several calcite precipitation events are missed, the lakes are still classified as lakes with calcite precipitation at other dates during our monitoring period. Extraordinary is the bright green color of Kleiner Glietzensee in March 2014 in the quasi-true color Landsat. Those two dates have been classified as calcite precipitation visually and automatically via Area BGR, but there is no in situ data as evidence available.

Table 7. Confusion matrices of Landsat-derived calcite precipitation with visual classifications at Feldberg Lake District, Klocksin Lake Chain, and Rheinsberg Lake Region.

Region	TP	TN	FN	FP	Sum	Accuracy
Feldberg Lake District	429	115	28	4	576	0.94
Klocksin Lake Chain	408	29	2	2	441	0.99
Rheinsberg Lake Region	1862	52	54	0	1968	0.97

4.5. Frequency and Duration of Landsat-Derived Calcite Precipitation

Based on the Landsat classification results, we analyzed the frequency and duration of calcite precipitation. The results for each region are illustrated in Figure 14. A table that lists the classification results of all lakes and dates can be found in the Appendix A (Table A1).

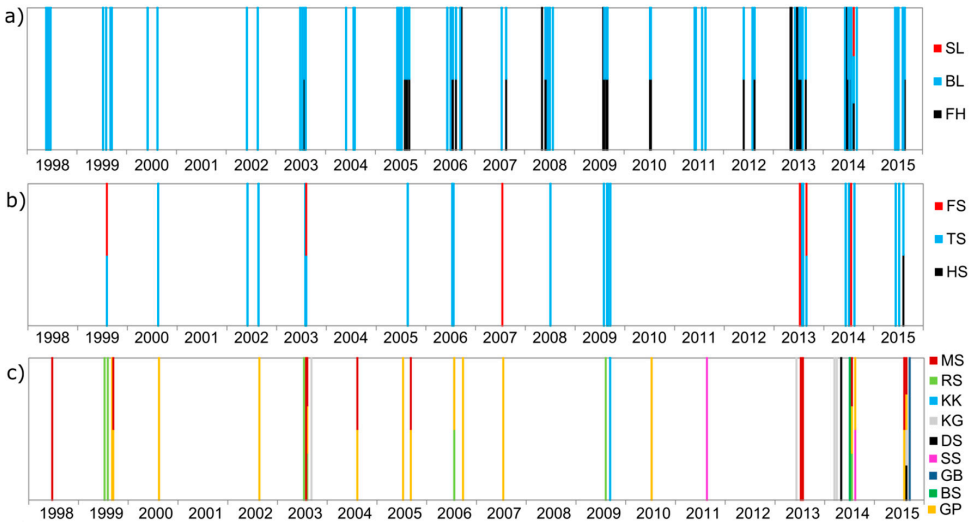

Figure 14. Frequency and duration of Landsat-derived calcite precipitation events at the study areas (1998–2015, cf. Appendix A). Images with calcite precipitation are illustrated as bars. (**a**) The Feldberg Lake District with FH, BL, and SL; (**b**) the Klocksin Lake Chain with Flacher See (FS), Tiefer See (TS), and Hofsee (HS); and (**c**) the Rheinsberg Lake Region with Menowsee (MS), Roofensee (RS), Kleiner Krukowsee (KK), Kleiner Glietzensee (KG), Dagowsee (DS), Stechlinsee (SS), Großer Boberowsee (GB), Breutzensee (BS) and Großer Paelitzersee (GP). When more than one lake shows calcite precipitation at the same date, the bars of the lakes are stacked.

4.5.1. Feldberg Lake District

In all lakes in Feldberg Lake District calcite precipitation events are detected (Figure 14a). All events occur between May and end of September. In FH regular calcite precipitation first occurred in 2005. Between 2005 and 2010 FH had regular calcite precipitation events. In 2011 no calcite precipitation occurred, but in the following three years regular calcite precipitation reoccurred. In 2015, there was only a single calcite precipitation event. BL has calcite precipitation every year except in 2001, but this year only had two Landsat acquisitions on 13 May 2001 and 20 October 2001. At SL one event was detected on the Landsat image on 13 August 2014.

For the calculation of durations, we excluded events which are only detected in one Landsat image, so called "single events". The maximum duration at FH is then 32 days, with an average duration of 24 days (standard deviation: 11 days). The maximum duration at BL is then 96 days, with an average duration of 57 days (standard deviation: 26 days). An example for a single event is FH in 2013: calcite precipitation was classified on 30 July 2003, but the acquisitions 16 days earlier and 16 days later both show a dark lake without calcite precipitation. This Landsat-derived classification results is equal to the visual classification. Generally, FH and BL show "start–stop–new–start–stop" temporal pattern: Acquisitions with Landsat-derived calcite precipitation are interrupted by acquisition without calcite precipitation, in 2013 in FH, and 2014 for both lakes. However, the visual classification differs from the Landsat-derived "start–stop–new–start–stop" at FH in 2014: The two of the five dates at FH between 4 July 2014 and 13 August 2014 that are classified as dates without calcite precipitation are classified visually as calcite precipitation and as bad quality images.

4.5.2. Klocksin Lake Chain

In three of the four lakes of the Klocksin Lake Chain, calcite precipitation events are detected (Figure 14b). At BS no calcite precipitation events were derived from the Landsat-images in the monitoring period. At HS one event was classified on 7 August 2015.

For FS calcite precipitation events are detected on individual Landsat images in 1999, 2003, 2007 and 2014. In 2013 there are three consecutive Landsat-derived events on 8 July 2013, 9 July 2013, and

48 days later, on 26 August 2013. TS shows the most frequent calcite precipitation events (in 11 of the 18 monitored years), whereas sediment analyses show either one or two thinner calcite layers every year. The selection of events in at least two consecutive acquisitions leaves seven years with long-lasting calcite precipitation events: the maximum duration is 56 days, the average is 31 days (standard deviation: 17 days).

4.5.3. Rheinsberg Lake Region

In nine of the 17 lakes in Rheinsberg Lake Region calcite precipitation is derived from Landsat images (Figure 14c). The lakes without calcite precipitation are Peetschsee, Großer Glietzensee (Ost), Großer Glietzensee (West), Großer Krukowsee, Nehmitzsee (north and south), Plötzensee, and Gerlinsee. In each one image Großer Boberowsee and Kleiner Krukowsee are classified as lakes with calcite precipitaion. Breutzensee, Dagowsee, and Stechlinsee have each two acquisitions that show calcite precipitation events. Only Kleiner Glietzensee, Roofensee, Menowsee, and Großer Pälitzsee show frequent calcite precipitation events on six to 18 dates. However, because of the high number of FN results, we renounced the calculation of durations. Extraordinary are two calcite precipitation events classifications in March at Kleiner Glietzensee (13 March 2014 and 30 March 2014).

4.6. Sentinel-2-Derived Calcite Precipitation in the Feldberg Lake District

Finally, we tested the Area BGR classification approach on a Sentinel-2 data set. Figure 15 illustrates the two existing Sentinel-2 images in 2015 and the contemporary Landsat images, together with their lake reflectance spectra.

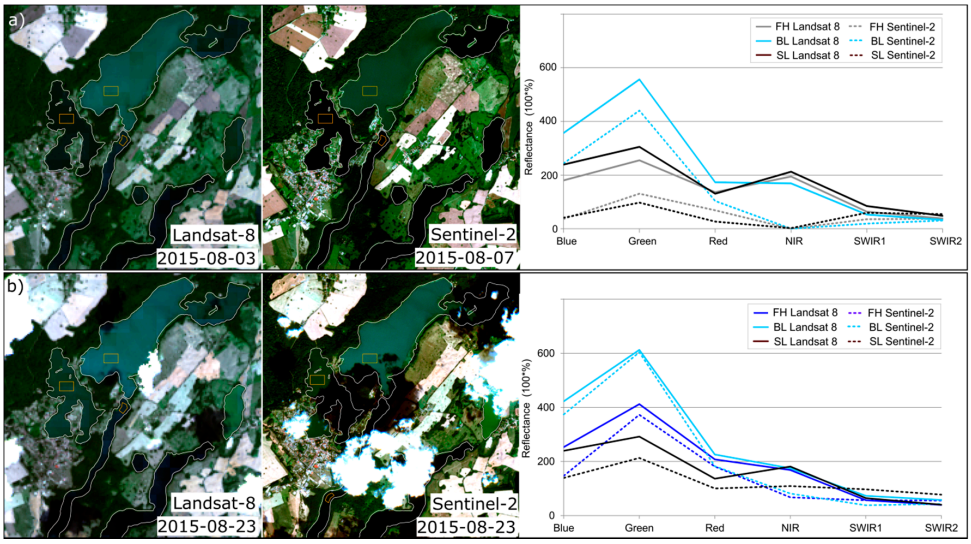

Figure 15. Comparison of two contemporary acquired quasi-true color RGB Landsat 8 and Sentinel-2 images of Feldberg Lake District (left and middle) and their according mean spectra (right side). In (**a**), the Landsat image was acquired on 3 August 2015; and the Sentinel image on 7 August 2015, in (**b**) both images are acquired on 23 August 2015. The orange rectangles in FH, BL and SL illustrate the ROI for the extraction of the mean reflectance spectra. Landsat spectra are illustrated as solid lines, Sentinel spectra as dotted lines.

On 7 August 2015 BH has calcite precipitation, on 23 August 2015 BL and FH. The lakes with calcite precipitation are in the Sentinel-2 images also characterized by a higher reflectance in comparison to the dark lakes without calcite precipitation. On both dates the Sentinel-2 images have lower reflectance values in the visible and NIR wavelength range than Landsat 8. The deviation is largest in the NIR band.

The classification of the Sentinel-2 images via threshold 13×10^3 of Area BGR shows the following results: On 3 August 2015, BL is classified as calcite precipitation with an Area BGR of 22.8×10^3.

FH (Area BGR: 7.0 $\times$ 10^3) and SL (5.5 $\times$ 10^3) are classified as lake without calcite precipitation. On 23 August 2015, BL (27.8 $\times$ 10^3) and FH (18.4 $\times$ 10^3) are classified as calcite precipitation, whereas SL (8 $\times$ 10^3) is classified as lake without calcite precipitation. The classification results of the Sentinel-2-derived classifications are equal to the Landsat-derived classification results and the confusion matrices of the Sentinel-2-derived classifications with the Landsat-derived classification and with the visual classification show a perfect accuracy of 1.00.

5. Discussion

5.1. Visibility of Calcite Precipitation in Multi-Spectral Satellite Imagery (Landsat and Sentinel-2)

The atmospheric correction is the most complex and error-prone processing step in water remote sensing as atmospheric correction models try to remove a large noise (atmosphere) from the small signal of water. However, in time series analysis atmospheric correction is essential for the comparison of different dates and sensors. In this study, we use the Landsat archive (Landsat 5, 7 and 8) and Sentinel-2 imagery, but the focus is the fast and easy applicability of satellite images for the monitoring of calcite precipitation. Thus, we ordered the satellite images in their highest processing level, including atmospheric correction, or used the state-of-the-art processor (e.g., sen2cor for the atmospheric correction) recommended by the provider of the satellite data. However, the models for the atmospheric correction differ for the different sensors and cause significant variation in the lake spectra (cf. Figure 13).

Despite the significant variation in the lake spectra, calcite precipitation events are clearly visible in multispectral Landsat and Sentinel-2 images. Whereas lakes without calcite precipitation appear black in quasi-true color RGB images, high $CaCO_3$ concentrations cause an additive effect to the spectra, especially in the green band, resulting in a turquoise color. In addition to calcite precipitation, the lake spectra can be influenced by other suspended minerals, yellow substances ("Gelbstoff"), and phytoplankton (chl-a concentration).

Other suspended mineral particles can increase the reflectance similar to calcite precipitation, but sediment entry is negligible in this study area because of dense vegetation cover, low topography and slow flow velocities that cannot carry sediments [2]. In other study areas, however, sediment entry might distort the monitoring of calcite precipitation. Another possible source of error are shallow water areas where the lake bottom can be seen or where wind can resuspend sediments that cause high particle concentrations in the open water [2]. Thus, the lake spectra for the analysis are extracted in deep areas of the lakes to avoid misclassifications.

Yellow substances ("Gelbstoff") in the water absorb in ultraviolet and blue [2,10,11], however, as colored dissolved organic matter (CDOM) was not measured in situ, we cannot estimate its influence on our lake spectra.

Whereas lakes with calcite precipitation are mostly turquoise, on some dates, the lake color appears more greenish than turquoise or is even bright green color (e.g., FH on 1 June 2008). Those green colors can be explained by (a mixture of calcite precipitation and) high chl-a concentrations: Phytoplankton scatters diffusely within the algal biomass (additive effect to the spectra), but also absorbs in blue and red [10,56,57]. Lake spectra with high chl-a are characterized by an peak around 700 nm (red edge) [56]. This peak cannot be detected using Landsat imagery because of the missing red-edge band of the Landsat sensors [42,43]. The new Sentinel-2 mission has a red-edge band and first tests with Sentinel-2 images showed its potential for the estimation of chl-a [58]. Thus, we expect that Sentinel-2 will be used in future for additional distinction between calcite precipitation and algal blooms. Even though in this study, the limited amount of Sentinel-2 data and a lack of contemporary in situ measurements hindered a further analysis.

Thus, in this study calcite precipitation and phytoplankton blooms cannot be distinguished clearly. The potential risk of misclassification in the lakes in Feldberg Lake District or Klocksin Lake Chain is very low because the lakes are mostly mesotrophic and considerable algal blooms are most likely in eutrophic lakes with chl-a concentration above 20 µg/L [56]). In Rheinsberg Lake Region,

several lakes are eutrophic and, whereas calcite precipitation events also occur in eutrophic lakes (cf. Feldberger Haussee), occasional misclassifications of algal blooms cannot be excluded (e.g., March 2014 at Kleiner Glietzensee).

5.2. Classification and Validation of Calcite Precipitation Using Multi-Spectral Satellite Imagery

Even though previous studies highlighted the patchiness of calcite precipitation in large lakes (area >20 km^2) [1,2,25], the lake colors in our study area are homogeneous (cf. Figures 2 and 9) as the smaller size of the lakes in northeastern Germany supports mixing processes. The only exceptions are different lake colors in separated basins of lakes (cf. BL in Figures 9d and 15). Some heterogeneity within the water bodies is smoothed out by the 30-m resolution of Landsat, but there are also artifacts from the atmospheric correction of Landsat 8 images that cause some variation [59]. Thus, in this study, a classification based on mean lake spectra was chosen to minimize the variation of the lake spectra. In other regions with higher heterogeneity classifications on pixel level might be preferable.

Thiemann and Koschel proposed a classification of calcite concentration based on 800 nm in hyperspectral images and considered more than 3% reflectance at 800 nm as calcite precipitation [2]. Although Landsat images do not have an 800 nm band, red is on average 655 nm and NIR is at 865 nm and a comparison with the spectra of BL (Figure 10) shows that only the strongest calcite precipitation on 11 July 1999 meets their criteria for calcite precipitation. At the other dates the reflectance of red and NIR are below 3% reflectance, even though in situ measurements showed increased $CaCO_3$ concentrations. Therefore, we tested several spectral indices for the classification of calcite precipitation. Best results were achieved with a classification based on the triangular area between the blue, green and red band in the spectra, the "Area BGR". If the Area BGR value is $\geq 13 \times 10^3$, the lake is classified as lake with calcite precipitation. This threshold is suitable for Landsat imagery and Sentinel-2 despite their differences in bandwidth and atmospheric correction.

Before this study, it was unknown which calcite concentrations were detectable from space. Thus, we compared our Landsat-derived classifications with different in situ $CaCO_3$ concentrations. Without optical aid a previous study suggested the limit for the visual detection of calcite precipitation is 1 mg/L [3]. Our classification approach was able to detect $CaCO_3$ concentrations $\geq$0.7 mg/L with an accuracy of 0.88. A higher threshold in the $CaCO_3$ concentration increases the number of FP classification results, whereas a lower $CaCO_3$ concentration increases the number of missed calcite precipitation events (=FN). The accuracy of the automatic classification is hereby also slightly better than the accuracy of the according visual classification of the quasi-true color RGB Landsat images (0.85).

The accuracy of the Landsat-derived classifications is decreased by FN and FP results: Here, FN results can be explained by the conservative threshold that is optimized for the correct classification of lakes without calcite precipitation: Thus, dates with only a slight color change are missed by the threshold. However, the six missed calcite precipitation events all have $CaCO_3$ concentrations between 0.95 and 1.65 mg/L which should have resulted in a visible color change. The visual classification of those dates confirms that four of the six dates indeed showed no or only a slight color change. The other two images have image quality problems and biased lake reflectance spectra because of cloud coverage. The lack in color change despite calcite precipitation might be explained by the heterogeneity of $CaCO_3$ concentrations within the lake or by time gaps of one day between in situ measurement and Landsat images. Thiemann and Koschel already noted the varying $CaCO_3$ concentrations within lakes in northeastern Germany and the possible problems for validation [2]. Despite careful work, measurement and transmission errors cannot be excluded for certain.

The nine FP classifications are related to already increased calcite concentrations between 0.41 and 0.69 mg/L and resulting in a turquoise color of the lakes. This applies specifically in the visual classification because of the high sensitivity of the human eye and thus a more sensitive visual classification. Because of the time gaps between in situ measurements and Landsat acquisition, it could also be that the concentration during the Landsat acquisition has already increased. An additional validation of single dates using the SI failed because of: (a) its short term changes as soon as

crystallization of $CaCO_3$ starts; and (b) its limitations in case of bio-induced calcite precipitation [17,18] as the occurrence of crystal nucleus, e.g., in form of bacteria [59,60], is equally important for calcite precipitation. Considering its SI FH has before 2011 not the potential for calcite precipitation, but in situ $CaCO_3$ measurements and the analysis of Landsat show clear calcite precipitation, whereas SL has high SI values since 2000 and therefore the potential for calcite precipitation, but still calcite precipitation events are very rare.

After the calibration and validation at Feldberg Lake District, the classificaion approach was applied in two other regions without in situ measurements. Here, the validation is based on visual classifications of the lakes. The accuracies are very high (0.99 and 0.97), but whereas Feldberg Lake District has a ratio of calcite precipitation events to normal lake conditions of 1:4, the ratio at Klocksin Lake Chain is already 1:14 and in Rheinsberg Lake Region even higher with 1:36. Thus, the accuracy is biased and in relation to the number of calcite precipitation events, the number of missed calcite precipitations (FN) is high in Rheinsberg Lake Region. The FN results can here also be explained by the conservative classification threshold in combination with the high sensitivity of the human eye and thus a more sensitive visual classification.

The accuracy based on the visual classification at Feldberg Lake District is 0.94. The lower accuracy at Feldberg Lake District in comparison to the other regions is caused by the less strict cloud removal. Especially, haze and missed cloud pixels hinder the accurate classification (FN results).

Whereas FN and FP classification results (e.g., FN results at lake Menowsee) distort the analysis of frequencies and durations, they do not affect the determination of the total area of lakes with calcite precipitation in this study. In comparison to the visual classification, FP are very rare, whereas all FN results occur at lakes that are, at other times, classified as lakes with calcite precipitation.

Overall, calcite precipitation events are detected in 15 of 24 lakes in the study areas and the total lake area of lakes with calcite precipitation is approximately 17 km^2. Thus, our study supports that calcite precipitation is a common phenomenon in the hardwater lakes, but it also emphasized that the durations and frequencies strongly vary so that each lake must be monitored individually.

5.3. Time Series: Frequency and Duration of Calcite Precipitation

Remote sensing data and especially, the large Landsat image archive, enable a long-term monitoring of large areas. However, for an accurate monitoring of the duration and frequency of calcite precipitation, a high acquisition density is required. The Landsat archives cannot provide a continuous temporal coverage, due to their limited repetition rate of 16 days and acquisition gaps by cloud coverage.

Whereas in some years with overlapping satellite missions the number of acquisitions is high, other years have only very few acquisitions, e.g., 2001 (cf. Figure 5). Since 2012, Landsat 7 and Landsat 8 are operating together providing a doubled repetition rate of eight days. However, cloud coverage still reduces the coverage significantly. For example, in 2012 the monitoring of the lakes in the Klocksin Lake Chain is only very irregular, because of the removal of cloud and cloud shadow (cf. Table A1). Thus, for a regular monitoring of calcite precipitation at selected lakes a less strict cloud and cloud shadow removal should be considered, even if this comes along with a higher number of misclassification because of cloud and haze (cf. classification accuracy of Feldberg Lake District). Earth observation with the Sentinel-2 satellite(s) will further increase the data density with its higher time resolution and repetition rate of 10 days. However, so far, only two Sentinel-2a images cover the study area, so that the full potential of Sentinel-2 could not yet be studied.

Calcite precipitation is known to be a spatial and temporal very variable process and it is linked to different factors, e.g., trophic state and occurrences of bacteria of the lakes. This causes changing calcite precipitation patterns in time and different calcite precipitation patterns even for adjacent lakes, e.g., in the Feldberg Lake District: even though SL was known for calcite precipitation before 1998, there were no calcite precipitation detected with in situ measurements after the lake restoration in 1996/1997. Whereas the in situ measurements between 1998 and 2015 show $CaCO_3$ concentrations <0.5 mg/L, the Landsat classification shows a clear calcite precipitation event on 13 August 2014

and misses further five visually classified calcite precipitation events. At FH, no calcite precipitation occurred before 2003. This fits to the in situ measurements: The long-term record (1985–2015) of mean seasonal (May–September) $CaCO_3$ concentration of FH indicates low values of <0.5 mg/L until 2005. Afterwards a substantial increase was observed. However, the reasons are not entirely clear. Koschel et al. (1983) have concluded that calcite precipitation might be most intensive in mesotrophic lakes [60]. By 2005 the seasonal (May–September) total phosphorus concentration of the mixed layer had dropped to 0.046 mg/L which is still in the eutrophic range but relatively close to mesotrophic conditions [61]. In 2011, when a second restoration measure has been carried out, calcite precipitation did not occur, while in 2012 a few calcite precipitation events and in 2013 several calcite precipitation events have been observed at FH. In 2014, the duration and frequency of calcite precipitation events is reduced again and in 2015 only one event has been observed. These variations can be explained by the complex process with competing inhibiting factors and supporting factors for calcite precipitation. During eutrophication phases, excess phosphorus has an inhibiting effect on calcite precipitation [12] so that artificial removal of phosphorous through poly-aluminum chloride might increase calcite precipitation. A follow-up monitoring will show if the restoration measures at FH have the same result (absence of calcite precipitation) as the restoration measures at SL.

The three lakes with the most calcite precipitation events are FH, BL, and TS. Their average durations are 24, 57, and 31 days (overall average: 37 day), but all three lakes show start–stop–start–stop patterns. However, the comparison of those patterns with the visual classifications reveals that most of those short-term variations are caused by misclassifications (e.g., FN results at FH between 4 July 2014 and 13 August 2014). Visually validated start–stop–start patterns, e.g., at FH between 24 July 2013 and 26 August 2013, substantiates the results of previous studies that showed calcite precipitation with lower calcite concentrations before and after the main event and non-steady, periodic variations [5].

Whereas the validation in Section 5.2 discusses the quality of the Landsat-derived calcite precipitation monitoring, it is still unknown, how many calcite precipitation events are missed in times without suitable satellite images or in situ measurements. Therefore, we included sediment analyses at TS to discuss the detection rate of calcite precipitation via remote sensing: The Landsat-derived monitoring at lakes in the Klocksin Lake Chain shows calcite precipitation events at TS at 11 of 18 years, whereas sediment analyses show calcite layers every year. A running monitoring study at TS using sediment traps shows high calcite deposition between May and September. The years 2001, 2007, 2010, and 2012 have only one or two Landsat acquisitions during May and September, thus calcite precipitation events were most likely missed. The years 1998, 2004, and 2011 have four, five, and nine acquisitions. However, the acquisitions are not equally distributed with maximum gaps of 55 days (2004 and 2011) to 89 days (1998) days between the acquisitions and thus, still calcite events could have happened in times without Landsat acquisitions. Especially, as the sediment layers in all of the missed years are extraordinary thin [33], which indicates either short-term or weak calcite precipitation events.

At region Rheinsberg Lake Region, eight of the 17 lakes show at least one calcite precipitation event, but the frequency of events is probably higher than our analyses shows, because the validation based on a visual classification reveals approximately as many calcite precipitation events as FN classifications. On the other hand, five lakes are eutrophic, thus, algal bloom may also occur, either contemporary to high $CaCO_3$ concentrations or independent of calcite precipitation. In this region the calcite precipitation on 20 August 2011 at the oligotrophic Stechlinsee has to be highlighted. This calcite precipitation is caused by storm "Otto" in July 2011, which caused the mixing of cyanobacteria populations from 7 m to 8 m depth into the surface water [28]. The resulting increase of the photosynthesis activity caused an increase of the $CaCO_3$ saturation index and lead to intensive calcite precipitation, still clearly visible in the Landsat image on 20 August 2011.

6. Conclusions

In this study, we tested the potential of the Landsat archive and Sentinel-2 for the classification and monitoring of calcite precipitation in lakes. Calcite precipitation due to increased $CaCO_3$ concentrations

cause an additive effect to the lake reflectance spectra, especially in the green band, resulting in quasi-true color RGB images in a turquoise color. Thus, we classify calcite precipitation events in lakes based on the calculation of the triangular area between blue, green and red in the mean lake spectra (Area BGR). We chose a conservative threshold, based on the comparison of visually turquoise and dark lake values of one lake (FH) for which a long-term in situ data archive of $CaCO_3$ concentrations is available. Overall, our study area covers 24 lakes. The classification results of FH, BL, and SL are validated with in situ measurements of calcite precipitation, for TS with sediment core data. We detected calcite precipitation with $CaCO_3$ concentrations $\geq$0.7 mg/L in the Feldberg Lake district with a good accuracy of 0.88. Our classification is here better than expected; a previous study suggested a limit of >1 mg/L.

The analysis of the false classified events showed that at some dates the lakes do not show a change of color even though the contemporary $CaCO_3$ concentration is high (FN classifications), whereas other dates with only slightly increased $CaCO_3$ values have a change of color (FP classifications). Important to consider is the time gap between in situ measurement and Landsat acquisition as well as a possible heterogeneous distribution of $CaCO_3$ in the lake.

In a next step, we tested the monitoring approach on 21 other lakes in the regions Klocksin Lake Chain and Rheinsberg Lake Region and validated the classification results based on a visual inspection of the Landsat data. Whereas FN results are relatively frequent in comparison to the number of detection calcite precipitation events, the overall accuracy in these two regions is still >0.97.

Our study shows that 15 of the 24 lakes covering a total area of approximately 17 km^2 have at least one calcite precipitation event in the observation period. The frequency of calcite precipitation events varies between one detection and regular detections nearly every year. The durations of calcite precipitation events also vary between the lakes, but are for the lakes with regular calcite precipitation (FH, BL, and TS) in average 37 days. The time series for Feldberg Lake District is denser than the one of Klocksin Lake Chain and Rheinsberg Lake Region, but has also a higher risk of misclassifications due to haze and remaining cloud pixels. However, still the effect of lake trophy restoration measures on calcite precipitation can be shown at SL and FH.

The high number of missed calcite precipitation events (=FN results), together with gaps in Landsat time series (e.g., 2001), reduces the accuracy of frequency and duration monitoring. For example, the comparison with sediment data at TS shows that calcite precipitation events have been missed in some years due to low image density in the critical time periods (May to September). In future the image density will increase by acquisitions of Sentinel-2a and coming Sentinel-2b. We tested the application of Area BGR classification method to Sentinel-2 and even although the sensors and the atmospheric correction differ, the classification approach is transferable. Another great potential of Sentinel-2 comes with its red-edge band: We expect that Sentinel-2 can also be used in future for the distinction between algal blooms and calcite precipitation.

Our results emphasized the variety of the lakes and the need to monitor each lake individually. This is due to the complex processes of calcite precipitation, which are influenced by a number of factors including lake trophic state, algae composition and activity, human measures and climate. Using the large Landsat archive and Sentinel-2 imagery, we now can provide an algorithm for monitoring calcite precipitation in lakes in the entire Northeast German Plain. This is an essential prerequisite, in combination with geochemical analyzes, to investigate the role of permanent CO_2 storage in form of calcite in this region.

Acknowledgments: This study was funded by the "Helmholtz Association of German Research Centres Initiative—Networking Fund for funding a Helmholtz Virtual Institute" (VH-VI-415).

Author Contributions: Iris Heine developed the methodological framework, performed programming, conducted the analysis and wrote the article; Peter Kasprzak and Ulrike Kienel provided in situ data for and contributed their expert knowledge on the study areas; Birgit Heim supported the analysis of the lake spectra based on her experience of water remote sensing; and Achim Brauer, Birgit Kleinschmit and Sibylle Itzerott were involved in formulating the research questions and contributing to critical discussions. All authors were involved in the general paper review.

Conflicts of Interest: The authors declare no conflict of interest.

Appendix A

Table A1. Calcite precipitation based on the Landsat time series (1998–2015) using the threshold of the area BGR. Lakes with calcite precipitation events are marked with "1" and highlighted in gray. Dark lakes without calcite precipitation are marked with "0". Blank cells are the dates without data.

Year	Date	Feldberger Haussee	Breiter Luzin	Schmaler Luzin	Bergsee	Hofsee	Tiefer See	Flacher See	Peetschsee	Dagowsee	Stechlinsee	Kleiner Glietzensee	Großer Glietzensee (Ost)	Großer Glietzensee (West)	Großer Boberowsee	Großer Krukowsee	Kleiner Krukowsee	Nehmitzsee South	Plötzensee	Breutzensee	Gerlinsee	Roofensee	Großer Pälitzsee	Nehmitzsee north	Menowsee
1998	26-March-1998	0	0	0	0	0	0	0	0	0	0	0	0	0	0	0	0	0	0	0	0	0	0	0	0
	13-May-1998	0	0	0	0	0	0	0	0	0	0		0	0	0	0	0	0	0	0	0	0	0	0	0
	20-May-1998	0	1	0					0	0						0		0	0						
	29-May-1998	0	1	0	0	0	0	0	0	0	0		0	0	0	0	0	0	0	0	0	0	0	0	0
	05-June-1998	0	1	0	0	0	0	0	0	0	0	0	0	0	0	0	0	0	0	0	0	0	0	0	0
	21-June-1998	0	1	0				0	0	0	0	0	0	0	0	0	0	0	0	0	0	0	0	0	1
	02-September-1998	0	0	0	0		0																		
1999	11-July-1999	0	1	0	0	0	0	0	0	0	0	0	0	0	0	0	0	0	0	0	0	1	0	0	0
	03-August-1999	0	1	0	0	0	1	1	0	0	0	0	0	0	0	0	0	0		0	0	1	0	0	0
	04-September-1999	0	1	0	0	0	0	0	0	0	0	0	0	0	0	0	0	0	0	0	0	0	1	0	0
	13-September-1999	0	1	0	0	0	0	0	0	0	0		0	0	0	0	0	0	0	0	0	0	1	0	1
	29-September-1999	0	0	0									0		0										
	15-October-1999	0	0	0	0	0	0		0	0	0		0	0	0	0		0	0	0	0	0	0	0	0
2000	19-January-2000	0	0	0	0	0	0				0			0				0						0	
	27-February-2000	0	0	0	0		0	0	0	0	0	0	0	0	0	0	0	0	0	0		0	0		0
	24-April-2000	0	0	0					0	0	0	0	0	0	0	0	0	0	0	0	0	0	0	0	0
	17-May-2000	0			0	0	0	0		0			0	0				0	0	0	0	0		0	
	02-June-2000	0	1		0	0	0	0	0	0	0							0	0	0					
	14-August-2000	0	1	0	0	0	1	0	0	0	0		0	0	0	0	0	0	0	0	0	0	1	0	0
	22-September-2000	0			0					0	0			0	0	0	0	0	0	0	0	0		0	0
	01-October-2000	0	0	0	0	0	0	0	0	0	0		0	0	0	0	0	0	0	0	0		0	0	0
	02-November-2000	0	0	0	0	0	0	0	0		0		0	0	0	0	0	0	0	0	0		0	0	0
2001	13-May-2001	0	0	0	0	0	0		0	0	0				0	0	0	0	0		0	0			
	20-October-2001	0	0	0		0			0				0	0	0	0	0					0	0	0	0
2002	29-March-2002	0	0	0	0	0	0	0	0	0	0	0	0	0	0	0	0	0	0	0	0	0	0	0	0
	05-April-2002	0		0																	0				
	21-April-2002	0	0		0	0	0	0	0	0	0	0	0	0	0	0	0	0	0	0	0	0	0	0	0
	01-June-2002	0	1	0	0	0	1	0		0	0					0	0								
	20-August-2002	0	1	0	0	0	1	0	0	0	0	0	0	0	0	0	0	0	0	0	0	0	1	0	0

Table A1. *Cont.*

Year	Date	Feldberger Haussee	Breiter Luzin	Schmaler Luzin	Bergsee	Hofsee	Tiefer See	Flacher See	Peetschsee	Dagowsee	Stechlinsee	Kleiner Glietzensee	Großer Glietzensee (Ost)	Großer Glietzensee (West)	Großer Boberowsee	Großer Krukowsee	Kleiner Krukowsee	Nehmitzsee South	Plötzensee	Breutzensee	Gerlinsee	Roofensee	Großer Pälitzsee	Nehmitzsee north	Menowsee
2003	23-March-2003	0	0	0	0	0	0	0		0	0	0	0		0	0	0	0	0	0	0	0	0	0	0
	17-April-2003	0	0	0	0	0	0	0	0	0	0	0	0	0	0	0	0	0	0	0	0	0	0	0	0
	28-June-2003	0	1	0	0	0	0	0	0	0	0		0	0	0	0	0	0	0	0	0	0	0	0	0
	14-July-2003	0	1	0				0												0	0	1		0	0
	30-July-2003	1	1	0	0	0	1	0	0	0	0		0	0	0	0	0	0	0	0	0	0	0	0	1
	06-August-2003	0	1	0	0	0	1	1	0	0		0		0	0	0		0	0		0	1	1	0	
	07-August-2003	0	1	0					0	0	0	0	0	0		0	0		0	0	0	1	1	0	1
	31-August-2003	0	0	0					0	0	0							0	0	0					
	07-September-2003	0	0	0					0	0	0	1	0	0	0		0								0
	16-September-2003	0	0	0	0				0	0	0		0	0	0	0	0	0	0	0	0	0	0	0	0
	02-October-2003	0	0	0	0	0		0																	
	17-October-2003	0	0	0	0	0	0	0	0	0					0		0	0		0	0	0		0	
	18-October-2003	0	0	0	0	0	0	0	0	0	0		0	0	0	0	0	0	0	0	0	0	0	0	0
2004	18-April-2004	0	0	0	0	0	0	0	0	0	0	0	0	0	0	0	0	0	0	0	0	0	0	0	0
	29-May-2004	0	1	0	0	0	0	0	0	0	0	0	0	0	0	0	0	0	0	0	0	0	0	0	0
	23-July-2004	0	1	0	0	0	0	0	0	0	0	0		0	0	0	0	0	0	0	0	0	0	0	0
	31-July-2004	0	1	0				0					0	0											0
	01-August-2004	0	1	0	0	0	0	0	0	0	0	0	0	0	0	0	0	0	0	0	0	0	0	0	0
	09-August-2004	0	0	0			0		0	0	0				0	0	0	0		0	0	0	1	0	1
	10-September-2004	0	0	0	0	0	0		0	0	0				0		0	0		0	0		0	0	
	11-October-2004	0	0	0	0	0		0		0		0	0	0	0	0		0		0					0
2005	21-March-2005	0	0	0	0	0			0		0	0			0		0	0	0	0		0	0	0	
	28- March -2005	0	0	0	0	0	0		0	0					0	0	0	0		0	0			0	0
	21-April-2005	0	0	0	0	0	0	0	0	0	0	0	0	0	0	0	0	0	0	0	0	0	0	0	0
	16-May-2005	0	0	0										0							0			0	
	09-June-2005	0	1	0				0			0		0	0	0		0	0	0				0		0
	16-June-2005	0	1	0					0								0				0				
	24-June-2005	0	1	0																		0			
	25-June-2005	0	1	0																					
	03-July-2005	0	1	0								0	0	0	0										
	10-July-2005	0	1	0	0	0	0	0	0	0	0	0	0	0	0		0	0	0	0	0	0	1	0	0
	11-July-2005	0	1	0				0	0	0	0	0	0	0		0			0	0	0			0	
	04-August-2005	1	1	0					0						0		0		0		0	0	0	0	0
	20-August-2005	1	1	0	0	0	1	0		0						0		0	0	0	0			0	
	05-September-2005	1	1	0	0	0	0	0	0	0	0		0	0	0	0	0	0	0	0	0	0	1	0	1

Table A1. *Cont.*

Year	Date	Feldberger Haussee	Breiter Luzin	Schmaler Luzin	Bergsee	Hofsee	Tiefer See	Flacher See	Peetschsee	Dagowsee	Stechlinsee	Kleiner Glietzensee	Großer Glietzensee (Ost)	Großer Glietzensee (West)	Großer Boberowsee	Großer Krukowsee	Kleiner Krukowsee	Nehmitzsee South	Plötzensee	Breutzensee	Gerlinsee	Roofensee	Großer Pälitzsee	Nehmitzsee north	Menowsee
	06-October-2005	0	0	0	0	0	0	0							0		0	0	0			0			
	07-October-2005	0	0	0	0	0	0	0	0	0	0		0	0	0	0	0	0	0	0	0	0	0	0	0
	14-October-2005	0	0	0							0														
	15-October-2005	0	0	0				0	0	0	0		0	0		0			0	0	0	0	0	0	0
	30-October-2005	0	0	0	0	0	0	0	0	0	0			0	0	0	0	0	0	0		0	0	0	0
	31-October-2005	0	0	0		0		0			0			0	0		0	0	0	0		0	0		
	17-April-2006	0	0	0														0	0	0	0			0	
	03-May-2006	0	0	0	0	0	0	0	0	0	0	0	0	0	0	0	0	0	0	0	0	0	0	0	0
	10-May-2006	0	0	0	0	0	0	0	0	0	0	0	0	0	0	0	0	0	0	0	0	0	0	0	0
	11-June-2006	0	1	0	0	0	0	0	0	0	0	0	0	0	0	0	0	0	0	0	0	0	0	0	0
	12-June-2006	0	1	0				0		0	0	0	0	0		0	0		0	0	0		0	0	0
	06-July-2006	0	1	0	0	0	0	0	0	0	0		0	0	0	0	0	0	0	0	0	0	0	0	0
	13-July-2006	1	1	0		0	1			0	0							0	0	0	0	0		0	
	21-July-2006	1	1	0		0						0		0	0			0	0			1			
2006	22-July-2006	1	1	0	0	0	1	0	0	0	0		0	0	0	0	0	0	0	0	0	1	1	0	0
	14-August-2006	1	1	0						0	0	0			0	0						0			0
	15-September-2006	0	1	0	0	0	0	0	0	0	0	0	0	0	0	0	0	0	0	0	0	0	0	0	0
	24-September-2006	1	0	0	0	0	0	0	0	0	0		0	0	0	0	0	0	0	0	0	0	1	0	0
	01-October-2006	0	0	0	0	0	0	0														0			
	09-October-2006	0	0	0	0	0	0	0		0				0		0	0		0	0	0			0	0
	10-October-2006	0	0	0	0	0	0	0	0	0	0		0	0	0	0	0			0	0		0	0	0
	17-October-2006	0	0	0	0	0	0	0	0	0	0			0	0	0	0	0	0	0	0	0	0	0	0
	03-November-2006	0	0	0	0	0			0	0	0				0		0	0		0	0	0	0	0	0
	27-March-2007	0	0	0				0	0	0	0	0	0	0	0	0		0	0				0		0
	12-April-2007	0	0	0	0	0	0		0	0	0	0	0	0		0	0	0	0	0	0	0	0	0	0
	28-April-2007	0	0	0		0			0	0	0		0		0	0	0	0		0	0	0	0	0	0
2007	06-May-2007	0	0	0				0					0					0	0	0		0			
	16-July-2007	0	1	0	0	0	0	1	0	0	0	0	0	0	0	0	0	0	0	0	0	0	1	0	0
	18-August-2007	1	1						0																
	11-September-2007	0		0		0							0	0	0										
	20-March-2008	0	0	0	0	0				0			0	0		0	0		0	0	0			0	0
	21-April-2008	0	0	0	0				0	0			0			0	0	0		0	0			0	0
2008	07-May-2008	1	0	0	0	0	0	0	0	0					0					0		0			0
	01-June-2008	1	1	0			0	0	0	0	0	0	0	0	0	0		0	0		0	0	0		0

Table A1. *Cont.*

Year	Date	Feldberger Haussee	Breiter Luzin	Schmaler Luzin	Bergsee	Hofsee	Tiefer See	Flacher See	Peetschsee	Dagowsee	Stechlinsee	Kleiner Glietzensee	Großer Glietzensee (Ost)	Großer Glietzensee (West)	Großer Boberowsee	Großer Krukowsee	Kleiner Krukowsee	Nehmitzsee South	Plötzensee	Breutzensee	Gerlinsee	Roofensee	Großer Pälitzsee	Nehmitzsee north	Menowsee
	08-June-2008	1	1	0	0	0	0	0			0	0	0	0	0	0			0						
	17-June-2008	0	1	0						0										0	0				
	03-July-2008	0	1	0	0	0	1		0	0	0		0	0		0	0		0	0	0		0	0	0
	26-July-2008	0	1	0	0	0	0	0				0	0	0	0				0						
	23-October-2008	0	0	0		0			0		0				0	0	0	0		0		0	0	0	0
	01-April-2009	0	0	0						0			0	0	0	0					0			0	0
	17-April-2009	0	0	0	0	0												0		0	0	0		0	
	24-April-2009	0	0	0	0	0	0	0		0	0	0	0	0		0			0	0	0			0	0
	10-May-2009	0	0	0		0				0		0	0	0					0	0					0
	19-May-2009	0		0	0						0									0	0	0		0	
	30-July-2009	1				0	1	0																0	
2009	06-August-2009	1	1												0										
	07-August-2009	1	1	0	0	0			0							0						1		0	
	23-August-2009	1	1	0			1		0		0		0	0		0			0		0			0	
	30-August-2009	1	1	0			1																		
	08-September-2009	0	0	0				0	0		0	0	0	0	0		1	0	0	0		0	0		
	16-September-2009	0		0	0	0	1	0	0	0	0		0	0	0			0	0	0	0	0	0	0	0
	24-September-2009	0	0	0													0								
	20-April-2010	0	0	0							0	0	0	0			0	0	0				0		
	29-May-2010	0	0	0	0				0	0			0		0	0	0	0		0	0	0		0	0
	30-June-2010	0	0	0					0						0			0				0			
2010	09-July-2010	1	1	0				0		0	0		0	0	0	0		0	0			0	1		0
	16-July-2010	1	1	0	0	0	0	0		0								0		0				0	
	11-Sptember-2010	0	0	0						0			0			0	0		0	0					0
	13-October-2010	0	0	0				0		0	0	0	0	0	0	0			0		0	0			
	30-March-2011	0	0	0					0	0	0	0	0	0	0	0	0	0	0	0	0	0	0	0	0
	22-April-2011	0	0	0	0	0	0	0	0	0	0	0	0	0	0	0	0	0	0	0	0	0	0	0	0
	23-April-2011	0	0	0			0		0	0	0		0	0		0	0		0	0	0		0	0	0
	30-April-2011	0	0	0	0	0	0		0	0			0		0	0	0	0		0	0	0		0	0
2011	01-May-2011	0	0	0	0	0	0	0		0	0			0	0	0	0	0	0	0	0	0	0	0	0
	08-May-2011	0	0	0	0	0	0	0	0	0	0	0	0	0	0	0	0	0	0	0	0	0	0	0	0
	09-May-2011	0	0	0			0		0	0	0		0	0		0	0		0	0	0		0	0	0
	02-June-2011	0	1	0	0	0	0	0	0	0	0		0	0	0	0	0	0	0	0	0	0	0	0	0
	10-June-2011	0	1	0		0			0	0	0		0	0	0								0		
	27-July-2011	0	1	0	0	0	0	0							0	0	0				0		0		

Table A1. *Cont.*

Year	Date	Feldberger Haussee	Breiter Luzin	Schmaler Luzin	Bergsee	Hofsee	Tiefer See	Flacher See	Peetschsee	Dagowsee	Stechlinsee	Kleiner Glietzensee	Großer Glietzensee (Ost)	Großer Glietzensee (West)	Großer Boberowsee	Großer Krukowsee	Kleiner Krukowsee	Nehmitzsee South	Plötzensee	Breutzensee	Gerlinsee	Roofensee	Großer Pälitzsee	Nehmitzsee north	Menowsee
	20-August-2011	0	1	0		0	0	0			1		0	0	0	0			0						
	06-September-2011	0	0	0	0		0	0	0								0								0
	29-September-2011	0	0	0	0	0	0	0		0						0	0		0	0	0	0		0	
	30-September-2011	0	0	0			0		0	0	0		0	0		0	0		0	0	0		0	0	0
	15-October-2011	0	0	0	0	0	0	0	0	0	0		0	0	0	0	0	0	0	0	0	0		0	0
	16-October-2011	0	0	0				0	0		0				0		0	0	0	0	0	0	0	0	
	23-October-2011	0	0	0	0	0	0	0		0	0	0		0		0			0	0	0			0	0
	16-April-2012	0	0	0	0	0	0																		
	02-May-2012				0		0	0							0										
	27-May-2012	1	1	0			0									0					0			0	
	12-June-2012	0	0	0																					
2012	19-June-2012	0	0	0						0										0	0			0	
	30-July-2012		1	0																					
	15-August-2012	1	1	0				0																	
	02-October-2012	0	0	0									0	0	0			0	0						
	18-October-2012	0	0	0				0			0		0	0	0		0	0	0				0		
	20-April-2013	0	0	0					0	0	0	0	0	0	0		0	0	0	0	0	0	0	0	0
	28-April-2013	0	0	0													0			0			0		0
	05-May-2013	0	0	0						0			0			0	0				0			0	0
	06-May-2013	1	0	0	0	0	0	0																	
	13-May-2013	1	0	0																		0			
	06-June-2013	0	0	0	0	0	0	0	0						0		0	0	0			0			
	07-June-2013	0	1	0	0	0		0	0	0	0	1	0	0	0	0	0	0	0	0	0	0	0	0	0
	23-June-2013	1																							
2013	08-July-2013	1		0	0		0	1	0						0		0	0	0	0		0			
	09-July-2013	1	1	0	0	0	0	1	0	0	0		0	0	0	0	0	0	0	0	0	0	0	0	1
	16-July-2013	1	1	0					0			0	0	0	0			0	0	0	0		1	0	0
	17-July-2013	1		0						0					0	0									0
	24-July-2013	1	1	0	0	0	1			0			0	0		0	0			0	0			0	1
	02-August-2013	0	1	0	0	0	1		0	0	0		0	0	0	0	0	0	0	0	0	0	0	0	0
	26-August-2013	1	1	0	0	0	1	1		0	0		0	0	0			0		0	0			0	0
	29-October-2013	0	0	0														0			0				
	13-November-2013	0	0	0	0			0	0						0		0			0				0	0
2014	25-January-2014	0	0				0		0		0				0							0	0		
	13-March-2014	0			0	0	0	0	0	0	0	1	0	0	0	0	0	0	0	0	0	0	0	0	0

Table A1. *Cont.*

Year	Date	Feldberger Haussee	Breiter Luzin	Schmaler Luzin	Bergsee	Hofsee	Tiefer See	Flacher See	Peetschsee	Dagowsee	Stechlinsee	Kleiner Glietzensee	Großer Glietzensee (Ost)	Großer Glietzensee (West)	Großer Boberowsee	Großer Krukowsee	Kleiner Krukowsee	Nehmitzsee South	Plötzensee	Breutzensee	Gerlinsee	Roofensee	Großer Pälitzsee	Nehmitzsee north	Menowsee
	30-March-2014	0	0	0				0			0	1	0	0	0		0	0	0				0		
	01-May-2014	0	0	0				0		1	0		0	0	0	0	0		0				0		
	17-May-2014	0	0	0													0								
	10-June-2014	0	1	0	0	0	1	0																	
	18-June-2014	1	0	0					0	0	0		0	0	0	0			0		0				0
	03-July-2014	1	1	0								0		0		0		0	0	1	0			0	
	04-July-2014	1	1	0	0	0	1		0	0	0		0	0		0	0		0	1	0		0	0	0
	11-July-2014	0	1	0																					
	19-July-2014	1	1	0	0	0	0	1	0	0	0		0	0	0	0	0	0	0	0	0	1	1	0	1
	27-July-2014	0	1	0				0			0		0	0	0	0			0						
	13-August-2014	1	1	1	0	0	1		0	0	1		0	0	0	0	0	0	0	0	0	0	1	0	0
	05-September-2014	0	1	0	0	0	0	0	0	0	0	0	0	0	0	0	0	0	0	0	0		0	0	0
	06-September-2014	0	0	0				0	0	0	0				0		0	0	0	0	0	0	0	0	0
	08-October-2014	0	0	0			0			0	0					0				0			0	0	0
	08-March-2015	0	0	0	0	0	0	0		0	0	0	0	0		0			0		0				0
	17-March-2015	0	0	0				0	0	0	0	0					0	0	0	0	0	0	0	0	
	10-April-2015	0	0	0	0				0	0	0	0	0	0	0	0	0	0	0	0	0	0	0	0	0
	04-June-2015	0	0	0	0	0	0		0	0	0	0	0	0	0	0	0	0	0	0	0	0	0	0	0
	05-June-2015	0	0	0	0	0			0	0	0		0	0	0	0	0	0		0	0	0	0	0	0
	12-June-2015	0	0		0		1	0							0		0	0		0	0			0	0
	13-June-2015	0	1	0				0																	
	28-June-2015	0	1	0							0		0	0	0	0			0						
	29-June-2015	0	1	0		0			0			0											0		0
	06-July-2015	0	1	0		0					0														0
2015	07-July-2015	0	1	0			1		0	0	0		0	0	0	0			0	0	0	0	0	0	0
	07-August-2015	0	1	0		1	1		0	0	0	0	0	0	0	0	0	0	0	0	0	0	1	0	1
	15-August-2015	0	1	0													0	0	0						
	23-August-2015	1	1	0		0		0	0	1	0	1	0	0	0	0		0	0	0	0		1	0	1
	08-September-2015					0		0		0	0	1					0	0	0	0	0		0	0	0
	17-September-2015	0	0	0	0				0	0	0		0	0	1	0	0	0		0	0	0	0	0	0
	03-October-2015	0	0	0	0	0	0	0	0	0	0		0	0	0	0	0	0	0	0	0	0	0	0	0
	10-October-2015				0	0	0	0																	
	11-October-2015	0	0	0			0		0	0	0		0	0		0			0	0	0		0	0	0
	26-October-2015	0	0	0	0	0	0	0	0	0	0			0	0	0	0	0	0	0	0		0	0	0
	27-October-2015	0	0	0			0		0	0	0			0	0	0					0	0	0		0

References

1. Strong, A.; Eadie, B.J. Satellite observations of calcium carbonate precipitations in the Great Lakes. *Limnol. Oceanogr.* **1978**, *23*, 877–887. [CrossRef]
2. Thiemann, S.; Koschel, R. Erfassung des räumlichen Verteilungsmusters von Kalkfällung mit Fernerkundungsdaten. *Wasser Boden* **2001**, *53*, 25–28.
3. Koschel, R.; Proft, G.; Raidt, H. Autochthone Kalkfällung in Hartwasserseen der Mecklenburger Seenplatte. *Limnologica* **1987**, *18*, 317–338.
4. Weidemann, A.D.; Bannister, T.T.; Effler, S.W.; Johnson, D.L. Particulate and optical properties during $CaCO_3$ precipitation in Otisco Lake. *Limnol. Oceanogr.* **1985**, *30*, 1078–1083. [CrossRef]
5. Proft, G. Die pelagische Calcitfällung und der Carbonatgehalt von Sedimenten pleistozäner Seen. *Acta Hydrochim. Hydrobiol.* **1984**, *12*, 321–326. [CrossRef]
6. Koschel, R.; Kasprzak, P.; Schreiber, A. Kalzitfällung und Nahrungskettenmanipulation. *Lauf. Semin.* **1997**, *3/97*, 61–76.
7. Kempke, S.; Schick, R.; Rinke, K.; Rothhaupt, K. Biogene Calcitfällung im Bodensee-Prozessverständnis und Modellierung. *WasserWirtschaft* **2008**, *98*, 31–33.
8. Hamilton, S.K.; Bruesewitz, D.A.; Horst, G.P.; Weed, D.B.; Sarnelle, O. Biogenic calcite–phosphorus precipitation as a negative feedback to lake eutrophication. *Can. J. Fish. Aquat. Sci.* **2009**, *66*, 343–350. [CrossRef]
9. Kelts, K.; Hsü, K. Chapter 9: Freshwater carbonate sedimentation. In *Lakes—Chemistry Geology Physics*; Springer: New York, NY, USA, 1978; pp. 295–323.
10. Kronberg, P. *Fernerkundung der Erde. Grundlagen und Methoden des Remote Sensing in der Geologie*; Enke Verlag: Stuttgart, Germany, 1985.
11. Fan, C. Spectral Analysis of Water Reflectance for Hyperspectral Remote Sensing of Water Quailty in Estuarine Water. *Water* **2014**, *2*, 19–27. [CrossRef]
12. Dittrich, M.; Koschel, R. Interactions between calcite precipitation (natural and artificial) and phosphorus cycle in the hardwater lake. *Hydrobiologia* **2002**, *469*, 49–57. [CrossRef]
13. Brunskill, G.J. Fayetteville Green Lake, New York. II. Precipitation and sedimentation of calcite in a meromictic lake with laminated sediments. *Limnol. Oceanogr.* **1969**, *14*, 830–847. [CrossRef]
14. Gal, J.Y.; Bollinger, J.C.; Tolosa, H.; Gache, N. Calcium carbonate solubility: A reappraisal of scale formation and inhibition. *Talanta* **1996**, *43*, 1497–1509. [CrossRef]
15. House, W. Inhibition of calcite crystal growth by inorganic phosphate. *J. Colloid Interface Sci.* **1987**, *119*, 505–511. [CrossRef]
16. Koschel, R. Structure and function of pelagic calcite precipitation in lake ecosystems. *Verh. Int. Ver. Limnol.* **1997**, *26*, 343–349.
17. Stabel, H.-H. Calcite precipitation in Lake Constance: Chemical equilibrium, sedimentation, and nucleation by algae. *Limnol. Oceanogr.* **1986**, *31*, 1081–1094. [CrossRef]
18. Thompson, J.B. Cyanobacterial Precipitation of Gypsum, Calcite and Magnesitre From Natural Lake Water. *Geology* **1990**, *18*, 995–998. [CrossRef]
19. Romero, L.; Camacho, A.; Vicente, E.; Miracle, M.R. Sedimentation patterns of photosynthetic bacteria based on pigment markers in meromictic Lake La Cruz (Spain): Paleolimnological implications. *J. Paleolimnol.* **2006**, *35*, 167–177. [CrossRef]
20. De Vicente, I.; Cattaneo, K.; Cruz-Pizarro, L.; Brauer, A.; Guilizzoni, P. Sedimentary phosphate fractions related to calcite precipitation in an eutrophic hardwater lake (Lake Alserio, northern Italy). *J. Paleolimnol.* **2006**, *35*, 55–64. [CrossRef]
21. Romero-Viana, L.; Julià, R.; Camacho, A.; Vicente, E.; Miracle, M.R. Climate signal in varve thickness: Lake la Cruz (Spain), a case study. *J. Paleolimnol.* **2008**, *40*, 703–714. [CrossRef]
22. Long, J.; Hu, C.; Robbins, L. Whiting events in SW Florida coastal waters: A case study using MODIS medium-resolution data. *Remote Sens. Lett.* **2014**, *5*, 539–547. [CrossRef]
23. Dierssen, H.M.; Zimmerman, R.C.; Burdige, D.J. Optics and remote sensing of Bahamian carbonate sediment whitings and potential relationship to wind-driven Langmuir circulation. *Biogeosci. Discuss.* **2008**, *5*, 4777–4811. [CrossRef]
24. Robbins, L.L.; Tao, Y.; Evans, C.A. Temporal and spatial distribution of whitings on Great Bahama Bank and a new lime mud budget. *Geology* **1997**, *25*, 947–950. [CrossRef]

25. Pulvermüller, A.G.; Kleiner, J.; Mauser, W. Calcite patchiness in Lake Constance as viewed by LANDSAT-TM. *Aquat. Sci.* **1995**, *57*, 338–349. [CrossRef]
26. Koschel, R.; Haubold, G.; Kasprzak, P.; Küchler, L.; Proft, G.; Ronneberger, D. Eine limnologische Zustandsanalyse des Feldberger Hausssees. *Acta Hydrochim. Hydrobiol.* **1981**, *9*, 255–279. [CrossRef]
27. Kasprzak, P.; Koschel, R.; Krienitz, L.; Gonsiorczyk, T.; Anwand, K.; Laude, U.; Wysujack, K.; Brach, H.; Mehner, T. Reduction of nutrient loading, planktivore removal and piscivore stocking as tools in water quality management: The Feldberger Haussee biomanipulation project. *Limnologica* **2003**, *33*, 190–204. [CrossRef]
28. Leibniz-Institute of Freshwater Ecology & Inland Fisheries (IGB). Unpublished Data, 2016.
29. Nixdorf, B.; Rücker, J.; Dolman, A.M.; Wiedner, C.; Hilt, S.; Kasprzak, P.; Köhler, A.; van de Klaus, W.; Sandrock, S.; Scharf, E.-M. Prozessverständnis als Grundlage für die Gewässerbewirtschaftung—Fallbeispiele für Limitation, Konkurrenz, Gewässerstruktur und Nahrungsnetzsteuerung. *Korresp. Wasserwirtsch.* **2013**, *6*, 693–701.
30. Nixdorf, B.; Hemm, M.; Hoffmann, A.; Richter, P. *Dokumentation von Zustand und Entwicklung der Wichtigsten Seen Deutschlands (Teil 2)*; Umweltbundesamt: Dessau-Roßlau, Germany, 2004.
31. Bachor, A.; Carstens, M.; Klitzsch, S.; Korczynski, I.; Lemke, G.; Mathes, J.; Müller, J.; Schenk, M.; Seefeldt, O.; Schöppe, C.; et al. *Gewässergütebericht Mecklenburg-Vorpommern 2003/2004/2005/2006: Ergebnisse der Güteüberwachung der Fließ-, Stand- und Küstengewässer und des Grundwassers in Mecklenburg-Vorpommern*; Landesamt für Umwelt, Naturschutz und Geologie: Güstrow, Germany, 2006.
32. Geodaten des Bundesamt für Kartographie und Geodäsie. Digitales Basis-Landschaftsmodell (Basis-DLM). Bundesamt für Kartographie und Geodäsie: Frankfurt, Germany, 2011. Available online: https://www.bkg.bund.de/DE/Produkte-und-Services/Shop-und-Downloads/DigitaleGeodaten/Landschaftsmodelle/Deutschland/DLMDeutschland_cont.html (accessed on 27 June 2011).
33. Kienel, U.; Dulski, P.; Ott, F.; Lorenz, S.; Brauer, A. Recently induced anoxia leading to the preservation of seasonal laminae in two NE-German lakes. *J. Paleolimnol.* **2013**, *50*, 535–544. [CrossRef]
34. Kienel, U.; Kirillin, G.; Brademann, B.; Plessen, B.; Lampe, R.; Brauer, A. Effects of the mixing duration in spring on diatom deposition in the deep Lake Tiefer See, NE Germany. *J. Paleolimnol.* **2016**, 1–13. [CrossRef]
35. Müller, J. GAIA-MV: Tiefenkarten der Seen in Mecklenburg-Vorpommern. Available online: http://www.geodaten-mv.de/ (accessed on 21 September 2016).
36. Spieß, H.-J. Ergebnisse der Untersuchungen submerser Makrophyten in mesotroph-eutrophen Seen Mecklenburg-Vorpommerns. *Rostock. Meeresbiol. Beitr.* **2004**, *13*, 73–84.
37. Nixdorf, B.; Hemm, M.; Hoffmann, A.; Richter, P. *Dokumentation von Zustand und Entwicklung der Wichtigsten Seen Deutschlands (Teil 5)*; Umweltbundesamt: Dessau-Roßlau, Germany, 2004.
38. Mietz, O.; Arp, W.; Riemer, A.; Vitinghoff, H.; Henker, H.; Wöbbecke, K.; Gabrysch, M.; Dahm, J.; Pausch, S.; Psille, D.; et al. *Seenkataster Brandenburg*; Bericht des Projektes; Die Seen im Land Brandenburg: Seddin, Germany, 1995.
39. Koschel, R. Leitbilder eines integrierten Seen- und Landschaftsschutzes. In *Stechlin-Forum*; Umweltstiftung WWF-Deutschland: Brandenburg, Germany, 1998; pp. 53–62.
40. Kabus, T.; Wiehle, I. Die Armleuchteralgen (Characeae) in ausgewählten Seen des Naturparks Stechlin-Ruppiner Land (Brandenburg, Deutschland). Ergebnisse der Untersuchungen außerhalb von FFH- und Naturschutzgebieten. *Rostock. Meeresbiol. Beitr.* **2013**, *24*, 63–74.
41. Kerstin, W.; Enviteam, B. *Badegewässerprofil Nach Artikel 6 der Richtlinie 2006/7/EG und § 6 der Verordnung über die Qualität und die Bewirtschaftung der Badegewässer vom 06.02.2008 (BbgBadV)*; Ministerium der Justiz und für Europa und Verbraucherschutz des Landes Brandenburg: Potsdam, Germany, 2008.
42. National Aeronautics and Space Administration (NASA). *Landsat 7 Science Data Users Handbook*; NASA: Washington, DC, USA, 2011.
43. Irons, J.R.; Dwyer, J.L.; Barsi, J.A. The next Landsat satellite: The Landsat Data Continuity Mission. *Remote Sens. Environ.* **2012**, *122*, 11–21. [CrossRef]
44. Drusch, M.; Del Bello, U.; Carlier, S.; Colin, O.; Fernandez, V.; Gascon, F.; Hoersch, B.; Isola, C.; Laberinti, P.; Martimort, P.; et al. Sentinel-2: ESA's Optical High-Resolution Mission for GMES Operational Services. *Remote Sens. Environ.* **2012**, *120*, 25–36. [CrossRef]
45. U.S. Department of the Interior; U.S. Geological Survey. USGS Website: Earthexplorer. Available online: http://earthexplorer.usgs.gov/ (accessed on 24 February 2016).

46. European Union. European Space Agency (ESA) for Earth observation Sentinels Scientific Data Hub. Available online: https://scihub.copernicus.eu/dhus/#/home (accessed on 6 June 2016).
47. European Space Agency (ESA) for Earth Observation. Sen2Cor Toolbox. Available online: http://step.esa.int/main/third-party-plugins-2/sen2cor/ (accessed on 6 June 2016).
48. European Space Agency (ESA) for Earth Observation. Sentinel-2 Toolbox. Available online: http://step.esa.int/main/toolboxes/sentinel-2-toolbox/ (accessed on 6 June 2016).
49. Hepperl, D.; Krienitz, L. Phacotus lenticularis (Chlamydomonadales, Phacotaceae) zoospores require external supersaturation of calcium carbonate for calcification in culture. *J. Phycol.* **1997**, *33*, 415–424. [CrossRef]
50. Hepperle, D. WinIAP—Software for the Calculation of Ion Activities and Calcite Saturation Index. SequentiX—Digital DNA Processing. Available online: http://www.sequentix.de (accessed on 29 April 2016).
51. Tucker, C.J. Red and Photographic Infrared Linear Combinations for Monitoring Veqetation. *Remote Sens. Environ.* **1979**, *8*, 127–150. [CrossRef]
52. McFeeters, S.K. The use of the Normalized Difference Water Index (NDWI) in the delineation of open water features. *Int. J. Remote Sens.* **1996**, *17*, 1425–1432. [CrossRef]
53. Xu, H. Modification of normalised difference water index (NDWI) to enhance open water features in remotely sensed imagery. *Int. J. Remote Sens.* **2006**, *27*, 3025–3033. [CrossRef]
54. Braden, B. The Surveyor's Area Formula. *Coll. Math. J.* **1986**, *17*, 326–337. [CrossRef]
55. Curran, P.J.; Dungan, J.L.; Peterson, D.L. Estimating the foliar biochemical concentration of leaves with reflectance spectrometry: Testing the Kokaly and Clark methodologies. *Remote Sens. Environ.* **2001**, *76*, 349–359. [CrossRef]
56. Thiemann, S.; Kaufmann, H. Determination of chlorophyll content and trophic state of lakes using field spectrometer and IRS-1C satellite data in the Mecklenburg Lake District, Germany. *Remote Sens. Environ.* **2000**, *73*, 227–235. [CrossRef]
57. Schultz, G.; Engman, E. *Remote Sensing in Hydrology and Water Management*; Springer: Berlin/Heidelberg, Germany, 2000.
58. Toming, K.; Kutser, T.; Laas, A.; Sepp, M.; Paavel, B.; Noges, T. First experiences in mapping lakewater quality parameters with sentinel-2 MSI imagery. *Remote Sens.* **2016**, *8*, 1–14. [CrossRef]
59. U.S. Department of the Interior; U.S. Geological Survey. *Product Guide—Provisional Landsat 8 Surface Reflectance Product*; Version 2.1.; U.S. Geological Survey: Sioux Falls, SD, USA, 2016. Available online: https://landsat.usgs.gov/landsat-surface-reflectance-high-level-data-products (accessed on 17 August 2016).
60. Koschel, R.; Benndorf, J.; Proft, G.; Recknagel, F. Calcite precipitation a a natural control mechnism of eutrophication. *Arch. Hydrobiol.* **2011**, *98*, 340–408.
61. Riedmüller, U.; Hoehn, E.; Mischke, U. *Trophieklassifikation von Seen. Richtlinie zur Ermittlung des Trophie-Index nach LAWA für natürliche Seen, Baggerseen, Talsperren und Speicherseen*; Bund/Länderarbeitsgemeinschaft Wasser (LAWA), Ed.; Kulturbuch-Verlag: Berlin, Germany, 2014.